

1 Article

2 Optimal Network Reconfiguration in Active 3 Distribution Networks with Soft Open Points and 4 Distributed Generation

5 Ibrahim M. Diaaeldin ¹, Shady H. E. Abdel Aleem², Ahmed El-Rafei ³, Almoataz Y. Abdelaziz ⁴
6 and Ahmed F. Zobaa ^{5,*}

7 ¹ Engineering Physics and Mathematics Department, Ain Shams University, Cairo, Egypt;
8 ibrahimmohamed@eng.asu.edu.eg; ibrahimmohamed@ieee.org

9 ² Mathematical, Physical and Engineering Sciences Department, 15th of May Higher Institute of
10 Engineering, Cairo, Egypt; engyshady@ieee.org; shossam@theiet.org

11 ³ Engineering Physics and Mathematics Department, Ain Shams University, Cairo, Egypt;
12 ahmed.elrafei@eng.asu.edu.eg

13 ⁴ Faculty of Engineering and Technology, Future University in Egypt, Cairo, Egypt;
14 almoataz.abdelaziz@fue.edu.eg; almoataz.abdelaziz@ieee.org

15 ⁵ Electronic and Computer Engineering Department, Brunel University London, Uxbridge UB8 3PH, U.K.;;
16 azobaa@ieee.org

17 * Correspondence: azobaa@ieee.org

18 Received: date; Accepted: date; Published: date

19 **Abstract:** In this study, we are motivated to allocate soft open points (SOPs) and distributed
20 generation (DG) units simultaneously with and without network reconfiguration (NR) and
21 investigate the contribution of SOP losses to the total active losses, as well as the effect of increasing
22 the number of SOPs connected to distribution systems under different loading conditions. A recent
23 meta-heuristic optimization algorithm called the discrete-continuous hyper-spherical search
24 algorithm is used to solve the mixed-integer nonlinear problem of SOPs and DGs allocation along
25 with new NR methodology to obtain radial configurations in an efficient manner without the
26 possibility of getting trapped in local minima. Further, multi-scenario studies are conducted on an
27 IEEE 33-node balanced benchmark distribution system and an 83-node balanced distribution
28 system from a power company in Taiwan. The contributions of SOP losses to the total active losses,
29 as well as the effect of increasing the number of SOPs connected to the system, are investigated to
30 determine the real benefits gained from their allocation. It was clear from the results obtained that
31 simultaneous NR, SOP and DG allocation into a distribution system creates a hybrid configuration
32 that merges the benefits offered by radial distribution systems and mitigates drawbacks related to
33 losses, power quality, and voltage violations while offering far more efficient and optimal network
34 operation. Also, it was found that the contribution of the internal loss of SOPs to the total loss for
35 different numbers of installed SOPs is not dependent on the number of SOPs and that loss
36 minimization is not always guaranteed by installing more SOPs or DGs along with NR. One of the
37 findings of the paper is demonstrating that NR with optimizing tie-lines could reduce active losses
38 considerably. As well, the results obtained validate, with proper justifications that SOPs installed
39 for the management of constraints in LV feeders, could further reduce losses and address issues
40 related to voltage violations and network losses efficiently.

41 **Keywords:** Distributed generation, load balancing, network reconfiguration, optimization, power
42 loss minimization, soft open points.

43 **Abbreviations:**

ADN	Active distribution network
B2B VSC	Back-to-back voltage source converter
BLP	Bi-level programming
CB	Capacitor bank
D-HSS	Discrete hyper-spherical search algorithm
DC-HSS	Discrete-continuous HSS algorithm
DG	Distributed generation
EA	Evolutionary algorithm
ESS	Energy storage system
HC	Hosting capacity
HSS	Hyper-spherical search algorithm
HSA	Harmony search algorithm
MHM	Modified honeybee mating
MINLP	Mixed-integer nonlinear programming
MISOCP	Mixed-integer second-order cone programming
NR	Network reconfiguration
PF	Power factor
PQ	Power quality
PSO	Particle swarm optimization
SOP	Soft open point
SOCP	Second-order cone programming
SC	Sphere-center
VSC	Voltage source converter
VD	Voltage deviation
VRE	Variable renewable energy
GA	Genetic algorithm

44 **Nomenclature:**

A_{loss}^{SOP}	Loss coefficient of VSCs
$AVDI$	Aggregate voltage deviation index
AP	The assigning probability
D_{sc}	Normalized dominance for each SC
$DSOF$	Difference of set objective functions for each set of particles and their sphere-center
f_{sc}	Objective function value for each SC
$f_{particles\ of\ sc}$	Objective function value for each particle assigned to a SC
I_b	line current flowing in line b
I_b^{rated}	Rated line current flowing in line b
LBI_b	Load balancing index of line b
LBI_{tot}	Total load balancing index
Max_{iter}	Maximum number of iterations
M	Incidence matrix
N_{br}	Number of lines existing in the distribution network
N_n	Number of nodes existing in the distribution network
N_f	Number of feeders

N_{DG}	Number of distributed generators
N_{SOP}	Number of allocated SOPs
N_{pop}	Population size
N_{SC}	Number of sphere-centers
N_{newpar}	Number of new generated particles
N	Number of decision variables
OFD	Objective function difference
Pr_{angle}	Probability of changing particle's angle
P_i, Q_i	Active and reactive power injected at the i^{th} node
P_i^L, Q_i^L	Active and reactive power of the connected load to the i^{th} node
P_i^{DG}, Q_i^{DG}	Active and reactive DG power injected at the i^{th} node
P_i^{SOP}, Q_i^{SOP}	SOP active and reactive power injected to the I^{th} feeder
$P_i^{SOP-loss}$	Internal power loss of the converter connected to the I^{th} feeder
P_{loss}^{tot}	Total active power losses
$p^{SOP-loss}$	SOP's internal power losses
$Q_i^{SOP-min}, Q_i^{SOP-max}$	Minimum and maximum SOP reactive injected to the I^{th} feeder
$r_{i,i+1}, x_{i,i+1}$	Line resistance and reactance between nodes i and $i + 1$
r, θ	Distance and angle between the particle and the sphere-center
r_{min}, r_{max}	Minimum and maximum radius of the sphere-center for continuous HSS
$r_{d,min}, r_{d,max}$	Minimum and maximum radius of the sphere-center for discrete HSS
S_i^{SOP}	Maximum capacity limit of the planned SOP
S^{DG}	Maximum capacity limit of the installed DGs
SOF	Set objective function
μ	Binary variable set to 1 if the SOP loss is considered and to 0 if the SOP loss is not considered.
$ V_i $	Magnitude of the voltage at the i^{th} node
V_{min}, V_{max}	Minimum and maximum voltage limits
X_{rand}	Random binary vector
X_{temp}	Temporary binary vector
D_{temp}	A vector equal to the difference between the temporary and random vectors
X_{check}	Reconfiguration checking vector
X_{best}^{rec}	Best reconfiguration vector
x_i	A vector of decision variables
$X_{i,min}, X_{i,max}$	Minimum and maximum values of continuous decision variables
$X_{id,min}, X_{id,max}$	Minimum and maximum values of discrete decision variables
β_{min}	Minimum lagging power factor

45 1. Introduction

46 The high penetration of distributed generation (DG) units has resulted in new challenges for the
47 planning and operation of power distribution systems, such as power loss increase, harmonic
48 distortion aggregation, equipment overloads, and voltage quality problems. Thus, there is significant

49 room for improvement and new perceptions to face these challenges are needed to cope with future
50 advances in order to realize resilient electrical distribution systems with high renewables penetration
51 and guarantee reliable and efficient network performance. In this regard, transmission and
52 distribution network operators are facing a great challenge to identify the sources of network losses,
53 utilize appropriate solutions to ensure reduced losses, operational costs and emissions, while keeping
54 future energy losses as low as possible through proper planning of distribution systems with low
55 carbon technologies [1], [2]. Variable renewable energy (VRE) sources, as solar and wind, are
56 considered as alternative ways to these issues, providing sustainable, clean, and eco-friendly nature.
57 However, the success in implementing VREs integration into modern distribution grids considerably
58 depends on developments of the energy storage markets along with improved regulations to
59 motivate the increased use of energy storage systems with renewables [3].

60 *1.1. Motivation*

61 Traditionally, power loss can be minimized via several methods such as using power quality
62 (PQ) devices to enhance the PQ performance of a system by limiting inefficiencies in the way power
63 is transferred and reducing harmonic distortion, which result in increased loss in distribution
64 networks [4]; reducing network imbalance, as an unbalanced power system will have higher currents
65 in one or more phases compared to balanced power systems [5]; improving the power factor (PF)
66 where low PF circuits suffer from a significant increase in the current at the same power delivered
67 [6]; configuring power system networks to provide a flexible framework to transfer electrical loads
68 between feeders that result in minimized loss and improved balancing of loads [7]; upgrading
69 networks to higher voltage levels while expanding reinforcement plans to guarantee significant loss
70 savings [8], [9] considering enhanced demand response programs to reschedule energy usage and
71 improve the reliability and efficiency of electrical networks and consequently reduce losses [10]; and
72 allocating DG units and power electronic devices in the distribution network [11] to control power
73 delivery between interlinked feeders and reduce power loss efficiently. However, it is prudent to
74 ensure that DGs or electronic devices are optimally sized and connected to suitable locations in power
75 systems to take full advantage of their positive benefits [1], [7].

76 Power systems are electrically separated via open points (switches). These open points are
77 strategically positioned to balance loads and hence reduce losses. Hence, network reconfiguration
78 (NR) can be performed by changing the state of sectionalized (closed) and tie (open) switches,
79 considering the need not to lose the radiality of the system. In the literature, NR has been applied in
80 different works to minimize network losses, improve the voltage profile, balance loads between two
81 or more feeders, and reduce the need for network reinforcement, while considering the influence and
82 increase of penetration of the DG units [7]. Also, the NR problem can be solved while taking into
83 account the optimal placement of shunt capacitors [12], harmonic filters [13] and power electronic
84 devices [14] to control the flow of either reactive and active powers or both between the feeders they
85 are connected to, because the extra power conditioners may be beneficial in some cases to enhance
86 the operational flexibility of the existing configurations, leading to more cumulative benefits of
87 reduced losses.

88 *1.2. Literature Review*

89 In this regard, soft open points (SOPs) are power electronic devices that can be placed instead of
90 normally open/closed points to provide a fast response, frequent actions and enhanced control
91 scheme for power flow between adjacent feeders they are connected to. In the near past, the optimal
92 operation of SOPs was investigated in balanced and unbalanced active distribution networks [15],
93 [16]. Several design strategies are manipulated for their optimal operation, such as the minimization
94 of energy loss [17] or annual expense [18] in a system, loads balancing [19], voltage profile

95 enhancement [19], and increasing the renewables hosting capacity [20] in distribution systems.
96 Various single-objective and multi-objective optimization techniques were used to solve these
97 optimization problems. In [11], a multi-objective optimization problem is formulated to minimize
98 power losses, load balance and maximize DGs penetration using the pareto optimality. To fulfil this
99 aim, four DGs were optimally sized along with NR using the three objective functions individually.
100 However, the presented objectives were not optimally coordinated simultaneously using NR only as
101 the reverse powers were allowed causing successive DGs penetration and power losses increase.
102 After choosing the best configuration among the pareto solutions, a lossless SOP was optimally
103 allocated instead of a certain tie-line. SOP installation succeeded in minimizing power losses and load
104 balancing better than that obtained using NR only. Besides, the ability of the installed SOP to transfer
105 DGs injected powers from lower to heavy loaded feeders. The presented strategy was tested on the
106 IEEE-33-node distribution system only. In [21], a single objective optimization problem is formulated
107 as a MISOCP problem to minimize both the operational cost of distribution systems and ESS
108 investment cost. The proposed study was tested on the IEEE 33-node distribution system only. A
109 comparative study was demonstrated to discuss the advantages of applying individual strategies on
110 the energy storage systems (ESS) planning. The strategies include hourly NR, SOPs and DGs
111 allocation. Two types of DGs were adopted in this study, including DGs based inverters and DGs
112 operating at unity PF. DGs based inverters were better than unity PF DGs in decreasing the total cost.
113 Also, a short-term hourly NR incorporated to optimize the power flow problem and demonstrate its
114 benefits in the ESS planning. From this study, it was highly recommended to optimal size and site
115 SOPs and renewable DGs for better ESS planning. Table 1 presents an overview of research works
116 that have addressed SOPs design and operation [16]–[35].

117 Some researchers such as Xiao et al. [35] did not consider the active power loss of the SOP
118 although there is active power loss in the SOP itself. However, they assumed that the active power
119 loss of the SOP is relatively small when compared to the entire distribution system losses. On the
120 other hand, the impact of the internal active losses of SOPs was presented in many research works,
121 but the influence of SOPs' power loss on the system performance, its share in the total active power
122 loss, and the effect of increasing the number of SOPs connected to the system are not investigated in
123 these works. Also, throughout the literature, one can see that most of the studies concerned with NR
124 and SOPs assume a fixed number and location of the SOP, which might not result in optimal
125 operational performance, in addition to permitting reverse power flow in the systems considered in
126 these studies. Moreover, optimizing the NR, DGs allocation and SOPs placement strategies separately
127 has some drawbacks, such as the lack of collaboration between strategies, which may lead to sub-
128 optimal overall performance and an inability to model the correlation between the benefits of each
129 strategy. In [36], different strategies used for reducing power losses in the UK distribution systems
130 are introduced. The report presents comprehensive studies that have been carried out to investigate
131 losses drivers and to identify opportunities and strategies for reducing network losses through
132 improving system operation, system design, and deploying loss-reduction technologies in UK power
133 networks such as changes in network operational topology, improvement of power factor, changes
134 in load profile, controlling phase imbalance and harmonic distortion mitigation. One of the
135 interesting findings of the report was demonstrating that NR could reduce HV feeder losses by up to
136 15% in specific areas. As well, modeling demonstrated that SOPs, installed for the management of
137 constraints in LV feeders, could potentially reduce losses in the corresponding LV network by about
138 10%-15%. Besides, further reduction in losses could be achieved by optimizing tie-lines to consider
139 changes in demand, as presented in the manuscript.

140 To redress these gaps, in this study, we are motivated to allocate SOPs and DGs simultaneously
141 with and without NR and investigate the contribution of SOP losses to the total active losses, as well
142 as the effect of increasing the number of SOPs connected to the studied systems under different
143 loading conditions to determine the real benefits gained from each strategy. In addition, an analytical

144 NR approach is proposed to obtain radial configurations in an efficient manner without the
145 possibility of getting trapped in local minima. Further, multi-scenario studies, which aim to improve
146 the investigation of the overall performance of the strategies, are conducted on an IEEE 33-node
147 balanced benchmark distribution system and an 83-node balanced distribution system from a power
148 company in Taiwan. The multi-scenario studies investigated in this work are: 1) NR as a stand-alone
149 strategy, 2) DGs allocation as a stand-alone strategy, 3) simultaneous NR and DGs allocation, 4) SOPs
150 allocation without NR, 5) SOPs allocation after NR is performed, 6) simultaneous SOPs allocation
151 and NR, 7) simultaneous SOPs and DGs allocation without NR, 8) simultaneous SOPs and DGs
152 allocation after NR is performed, and 9) simultaneous NR and SOPs and DGs allocation.

153 A recent meta-heuristic optimization algorithm called the discrete-continuous hyper-spherical
154 search (DC-HSS) algorithm is used to solve the mixed-integer nonlinear problem (MINLP) of SOPs
155 and DGs allocation along with NR to minimize power loss in the distribution systems. The DC-HSS
156 has the advantages of fast convergence to the optimal/near-optimal solutions [39], [40].

157 **1.3. Contribution and Novelties**

158 The contribution of this work is twofold. First, we propose a new NR methodology to obtain the
159 possible radial configurations from random configurations to minimize power loss in two
160 distribution systems, taking into account different strategies for DGs, SOPs, and NR while
161 considering multi-scenarios to improve the investigation of the overall performance of the
162 strategies, and in turn their priorities. Second, the contribution of SOP losses to the total active losses
163 as well as the effect of increasing the number of SOPs connected to the system are investigated under
164 different loading conditions to determine the real benefits gained from SOPs and DGs allocation with
165 network reconfiguration to provide the best operation of distribution networks with minimum losses
166 and enhanced power quality performance. It was clear from the results obtained that placing SOPs
167 and DGs into a distribution system creates a hybrid configuration that merges the benefits offered by
168 radial and meshed distribution systems and mitigates drawbacks related to losses, PQ, and voltage
169 violations, while offering far more efficient and optimal network operation.

170 **1.4. Organization of the Paper**

171 The rest of the paper is organized as follows: Section II presents the problem statement, proposed
172 NR methodology, modeling of SOPs and DGs, and PQ indices that evaluate the system performance.
173 Further, Section III presents the problem formulation and the search algorithm used to solve the
174 mixed-integer nonlinear problem. Section IV presents the results and discusses them, and Section V
175 presents the conclusions and limitations of our study as well as a preview of future works.

176 **2. Materials and Methods**

177 The NR, SOPs and DGs modeling, and PQ performance indices, namely the load balancing index
178 (*LBI*), and aggregate voltage deviation index (*AVDI*), are presented and discussed. Hence, the
179 formulation of the load flow calculations, the objective function to minimize the network active
180 power loss, the constraint conditions of voltage, current, SOP capacity, active and reactive powers,
181 and the DC-HSS algorithm proposed to solve the formulated MINLP problem are presented.

Table 1. Overview of research works addressing SOPs design and operation

Ref.	Scope*	Year	Objective	Optimization technique	SOP	NR	DG	CB	ESS	OLTC	System	Remarks
[16]	PS	2016	Loss minimization and LBI	Improved Powell's Direct Set	√	√	√	×	×	×	33-node	A study was conducted to compare NR and SOP. A new methodology was proposed to combine NR and SOP.
[20]	PS	2017	HC maximization	Strengthened SOCP	√	×	√	×	×	×	33-node	A strengthened SOCP was proposed to verify the exactness of the optimality gap to maximize the HC of the system.
[30]	PE	2016	Studying the operation of SOPs	×	√	×	×	×	×	×	MV distribution network	The operating principles for the placement of SOPs under normal, fault and post-fault conditions were discussed.
[22]	PE	2018	Fault detection	×	√	×	×	×	×	×	×	A new index was proposed to detect faults based on local measurements of the symmetrical voltages.
[25]	PS	2017	Power loss minimization	PSO	√	×	√	×	×	×	Anglesey network	The main aim was to convert an existing double 33 kV AC circuit to DC operation to increase the HC of the network.
[23]	PS	2016	Annual costs minimization	MISOCP	√	×	√	×	×	×	33-node	A mixed-integer SOCP was proposed to minimize annual expenses, which comprise the investment cost of SOPs, operation cost of SOPs and power loss expenses.
[24]	PS	2017	DGs penetration maximization	Ant colony	√	√	√	×	×	×	33-node	Different scenarios were conducted to maximize DGs penetration.
[17]	PS	2017	Minimization of annual cost and power loss	BLP	√	×	√	√	×	×	33-node	Bi-level programming was used to find the optimal allocation of DGs, CBs and a SOP where the annual costs and power losses were considered as the problem levels.
[26]	PS	2019	Combined minimization of total power loss and VD	MISOCP	√	×	√	×	×	×	69-node and 123-node	A decentralization method was proposed to reduce the dependency on a massive communication and computation burden.
[27]	PS	2018	Power loss minimization	Sequential optimization	√	×	√	×	√	×	33-node	A new approach was introduced to gain the benefits of both SOPs and ESS. A sequential optimization model was used to minimize network losses, converter losses and ESS losses.
[28]	PS	2016	HC maximization	×	√	×	√	×	×	×	Generic system	HC maximization gained from insertion of a SOP between two distinct 33 kV networks were presented.

Ref.	Scope*	Year	Objective	Optimization technique	SOP	NR	DG	CB	ESS	OLTC	System	Remarks
[29]	PS	2016	Power loss minimization	MISOCP	√	√	√	×	×	×	33-node	A new methodology to allocate a SOP along with NR simultaneously considering the cost of switching actions and SOP losses was presented.
[21]	PS	2017	Minimization of ESS costs	MISOCP	√	√	√	×	√	√	33-node	Optimally sited and sized ESSs in an ADN that includes SOP and DGs smart inverters were presented.
[31]	PS	2017	LBI and power loss minimization	SOCP	√	×	√	×	×	×	33-node	Installation of a multi-terminal SOP using an enhanced SOCP-based method was proposed.
[32]	PS	2018	Restored loads maximization	Primal-dual interior-point	√	×	√	×	√	×	33-node and 123-node	SOP islanding partitioning of ADNs with DGs, loads and ESSs time series characteristics was presented.
[33]	PS	2017	Operation cost and VD minimization	MISOCP	√	×	√	√	√	√	33-node and 123-node	Optimal coordination between OLTC, CBs and SOP using a time-series model was presented.
[18]	PE	2016	VD, LBI and energy loss minimization	Interior-point	√	×	√	×	×	×	MV distribution network	A Jacobian matrix-based sensitivity method was proposed to operate a SOP under various conditions.
[19]	PS	2017	Power loss, LBI and VD minimization	MOPSO and Taxicab	√	√	√	×	×	×	69-node	Optimal allocation of SOP with NR at various DGs penetrations was presented.
[34]	PS	2017	Annual expenses minimization	MISOCP	√	√	√	×	×	×	33-node and 83-node	A new concept was presented to install SOPs in normally closed lines as well as normally open lines.
[35]	PS	2018	Voltage imbalance	Improved differential evolution algorithm	√	×	√	×	×	×	Hybrid distribution system	Optimal allocation of SOPs to improve 3-phase imbalance with DGs and loads uncertainties were proposed using an improved differential evolution algorithm.
Proposed	PS	2019	Power loss minimization	DC-HSS	√	√	√	×	×	×	33-node and 83-node	A simultaneous SOPs and DGs allocation along with NR is proposed. The proposed strategy was tested with/without SOPs loss consideration. Besides, a new NR methodology is proposed to provide resiliency in the distribution system power flow. Moreover, reverse powers are not permitted unlike previous works.

183 *PS denotes a power system perspective and PE denotes a power electronics perspective

184 2.1. Proposed Network Reconfiguration

185 Distribution systems have sectionalizing switches (normally closed switches) that connect line
 186 sections and tie switches (normally open switches) that connect two primary feeders, two substation
 187 buses, or loop-type laterals. Each line is assumed a sectionalized line with a normally closed
 188 sectionalized switch in the line. Also, each normally open tie switch is assumed to be in each tie line.
 189 Thus, NR is the change that occurs in the status of tie and sectionalized switches to reconnect
 190 distribution feeders to form a new radial structure for a certain operation goal without violating the
 191 condition of having a radial structure. In this study, the procedure of NR to generate possible radial
 192 configurations in a fast and efficient manner is implemented analytically and is clarified as follows:

193 **Step 1:** A binary vector $X_{rand}^{(0)} = [1\ 0\ 0\ 1\ 1\ \dots\ 1]_{1 \times N_{br}}$ is initialized with random binary values, in
 194 which its length is equal to the number of lines (N_{br}) with its sectionalized and tie switches. The
 195 sectionalized switches are denoted "1" and the tie switches are denoted "0".

196 **Step 2:** The best reconfiguration vector of the system (X_{best}^{rec}), which represents the best vector that
 197 meets the radiality requirements (described in Step 6) and achieves the desired goal, is initialized
 198 with the base configuration of the system.

199 **Step 3:** A temporary vector $X_{temp}^{(0)}$ that is equal to X_{best}^{rec} is created. At that point, each element in
 200 $X_{temp}^{(0)}$ is compared with the corresponding element in $X_{rand}^{(0)}$ to create a new vector $D_{temp}^{(0)}$ in which
 201 $D_{temp}^{(0)} = X_{temp}^{(0)} - X_{rand}^{(0)}$. Further, $\forall b \in N_{br}$, if $D_{temp}^{(0)}(b) = 1$, it means that this b th line is changed to
 202 a tie line in the random vector; also if $D_{temp}^{(0)}(b) = -1$, it means that the b th line is changed to a
 203 sectionalized line in the random vector. Otherwise, if $D_{temp}^{(0)}(b) = 0$, this indicates that no change has
 204 occurred.

205 **Step 4:** Starting from the first element in $D_{temp}^{(0)}$, if $D_{temp}^{(0)}(b) = 1$ and $D_{temp}^{(0)}(j) = -1$, where j
 206 denotes a random line selected from the remaining lines in the system with the condition that $b \neq j$,
 207 a vector $X_{check}^{(0)}$ is generated so that $X_{check}^{(0)}$ is equal to $X_{temp}^{(0)}$ subjected to $X_{check}^{(0)}(b) = 0$ and
 208 $X_{check}^{(0)}(j) = 1$. The vector $X_{check}^{(0)}$ is then checked for radiality described in Step 6. If it is found to be
 209 radial, then b is updated so that $b = b + 1$, and the vector $X_{temp}^{(1)}$ is generated equal to $X_{best}^{rec(1)}$. It
 210 should be mentioned that a set of $X_{check}^{(0)}$ vectors may be generated as soon as b is smaller than or
 211 equal to N_{br} , and the vectors found to be radial in this set are evaluated based on their fitness value
 212 to give the best X_{best}^{rec} .

213 **Step 5:** The steps will terminate when we achieve a very small distance among serial solutions by
 214 evaluation of the objective function.

215 **Step 6:** The procedure of radiality check is done as follows:

- 216 • Build an incidence matrix M where its rows and columns represent the lines and nodes of the
 217 distribution network, respectively. The nodes of each line are denoted "1" in M , and the rest of
 218 the elements in the row are denoted "0".
- 219 • Elements in the rows of each tie line are set to "0". Then, we create a vector S , in which its length
 220 is equal to the number of nodes, and each element e in S is equal to the sum of its corresponding
 221 e^{th} column in M . If an element in S is equal to "1", it means that this element represents an end
 222 node. Further, the row that corresponds to this end node in M is set to "0".
- 223 • Recalculate S and repeat the former process as soon as an element in S is equal to 1. At that
 224 point, calculate the sum of all the elements in M . If the sum is equal to zero, this means that the
 225 configuration is radial, otherwise, it is not radial.

226 2.2. SOP Modeling

227 SOPs were first presented in 2011 [41] to provide resilience between distribution feeders. They
 228 can be integrated in distribution networks using three topologies, comprising a back-to-back (B2B)
 229 voltage source converter (VSC), static series synchronous compensator and unified power flow

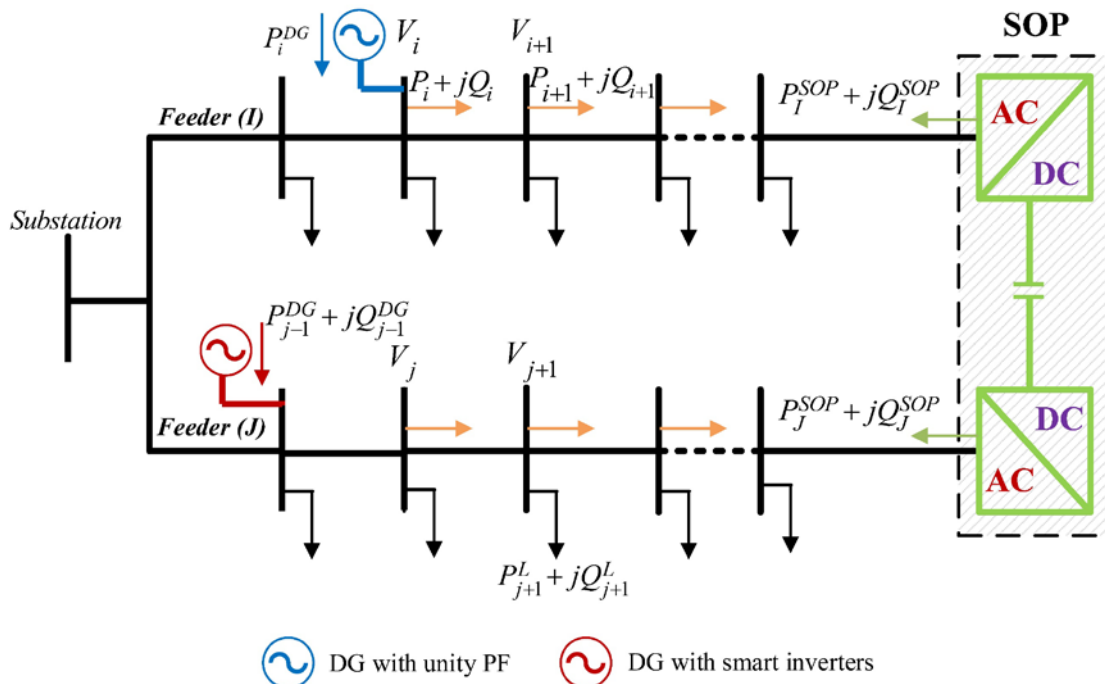
230 controller [42]. In this work, we used a B2B-VSC as the integration topology for SOPs connected to
 231 the studied systems because of its flexibility and dynamic capability to enhance the power quality.
 232 Fig. 1 shows an illustration of SOPs integration into a distribution system. To model a SOP, the main
 233 equations to model the flow of power in the network under study are expressed as follows [16]:

$$234 \quad P_{i+1} = P_i - P_{i+1}^L - r_{i,i+1} \cdot \frac{P_i^2 + Q_i^2}{|V_i|^2} \quad (1)$$

$$235 \quad Q_{i+1} = Q_i - Q_{i+1}^L - x_{i,i+1} \cdot \frac{P_i^2 + Q_i^2}{|V_i|^2} \quad (2)$$

$$236 \quad |V_{i+1}|^2 = |V_i|^2 - 2(r_{i,i+1} \cdot P_i + x_{i,i+1} \cdot Q_i) + (r_{i,i+1}^2 + x_{i,i+1}^2) \frac{P_i^2 + Q_i^2}{|V_i|^2} \quad (3)$$

237 where P_i and Q_i are the injected active and reactive powers at the i^{th} node, P_{i+1}^L and Q_{i+1}^L are the



238
 239

Figure 1. Illustration of SOPs integration into a distribution system

240 active and reactive powers of the connected loads onto node $i + 1$, $|V_i|$ is the magnitude of the i^{th}
 241 node voltage and $r_{i,i+1}$ and $x_{i,i+1}$ are the feeder resistance and reactance between nodes i +
 242 1.

243 Then, the SOP is integrated using its active and reactive powers injected at its terminals as
 244 presented in Fig. 1, in which the summation of the injected powers at the SOP terminals and the
 245 internal power loss of its converters must equal zero [16], as expressed in (4). Thus:

$$246 \quad P_I^{SOP} + P_J^{SOP} + P_I^{SOP-loss} + P_J^{SOP-loss} = 0 \quad (4)$$

247 The reactive power limits [16] are given in (5) and the SOP capacity limit [16] is shown in (6). Thus:

$$248 \quad Q_I^{SOP-min} \leq Q_I^{SOP} \leq Q_I^{SOP-max}, \forall I, J \in N_f \quad (5)$$

$$249 \quad \sqrt{(P_I^{SOP})^2 + (Q_I^{SOP})^2} \leq S_I^{SOP}, \forall I \in N_f \quad (6)$$

250 where N_f is the number of feeders, P_I^{SOP} is the SOP's active power injected to the I^{th} feeder, P_J^{SOP}
 251 is the SOP's active power to the J^{th} feeder, $P_I^{SOP-loss}$ is the active power loss of the converter
 252 connected to the I^{th} feeder, $P_J^{SOP-loss}$ is the internal power loss of the converter connected to the
 253 J^{th} feeder, Q_I^{SOP} is the SOP's reactive power injected to the I^{th} feeder, Q_J^{SOP} is the SOP's reactive
 254 power injected to the J^{th} feeder, $Q_I^{SOP-min}$ and $Q_I^{SOP-max}$ are the minimum and maximum limits
 255 of the SOP's reactive power injected to the I^{th} feeder, and S_I^{SOP} is the maximum capacity limit of
 256 the planned SOP. Further, the active loss of each converter ($P_I^{SOP-loss}$ and $P_J^{SOP-loss}$) and the total
 257 SOPs active power loss ($P^{SOP-loss}$) are formulated in (7) and (8) as follows [43]:

$$258 \quad p_i^{SOP-loss} = \sum_{l=1}^{N_f} p_l^{SOP-loss} \quad (7)$$

$$259 \quad p_i^{SOP-loss} = A_{loss}^{SOP} \sqrt{(P_i^{SOP})^2 + (Q_i^{SOP})^2}, \forall i \in N_f \quad (8)$$

260 where A_{loss}^{SOP} is the loss coefficient of VSCs, which represents leakage in the transferred power to the
261 total power transferred between feeders [33],[43]-[44].

262 Mathematically, to represent the SOP variables, first, we can consider a lossless SOP, i.e.
263 $p_i^{SOP-loss} = 0, \forall i \in N_f$; hence, a SOP can be represented by its injected active and reactive powers
264 $(P_i^{SOP}, Q_i^{SOP}, Q_j^{SOP})$, where $P_j^{SOP} = -P_i^{SOP}$. Therefore, multiple SOPs can be modeled by the vector
265 $[P_i^{SOP}(1), Q_i^{SOP}(1), Q_j^{SOP}(1), \dots, P_M^{SOP}(n), Q_M^{SOP}(n), Q_K^{SOP}(n)]$ such that the first three variables in the
266 vector represent the first SOP connected between the l th and J th feeders, while the last three variables
267 represent the n th SOP connected between the M th and K th feeders.

268 Second, we can consider the SOP with its losses taken into account, i.e. $p_i^{SOP-loss} \neq 0, \forall i \in N_f$;
269 hence, starting from (4), we can get $p_i^{SOP-loss}$ as follows:

$$270 \quad p_j^{SOP} = -P_i^{SOP} - p_i^{SOP-loss} - p_j^{SOP-loss} \quad (9)$$

271 Substituting (8) into (9), then

$$272 \quad p_j^{SOP} = -P_i^{SOP} - A_{loss}^{SOP} \sqrt{(P_i^{SOP})^2 + (Q_i^{SOP})^2} - A_{loss}^{SOP} \sqrt{(P_j^{SOP})^2 + (Q_j^{SOP})^2} \quad (10)$$

273 Accordingly, if we set P_i^{SOP}, Q_i^{SOP} and Q_j^{SOP} as the SOP's decision variables, (10) will be a
274 nonlinear equation with one unknown (P_j^{SOP}). So, it can be independently solved using numerical
275 analysis methods such as Newton's method to find the value of the root (P_j^{SOP}) of (10). Therefore,
276 assuming that A_{loss}^{SOP} is known; a SOP can be represented by its injected active and reactive powers
277 $(P_i^{SOP}, Q_i^{SOP}, Q_j^{SOP})$ as the lossless SOP case.

278 2.3. DG Modeling

279 In this study, we used two types of DGs. The first type includes generators with unity power
280 factor and the second is DGs with smart inverters [21] with a reactive power compensation capability
281 within specified limits of the reactive power.

282 The DGs with unity PF are limited by the maximum capacity limit (S^{DG}) of the installed DGs as
283 follows:

$$284 \quad 0 \leq P_i^{DG} \leq S^{DG} \quad (11)$$

285 where P_i^{DG} is the active DG power injected at the i^{th} node.

286 In the second type of DG, the reactive power varies based on specified PF limits, so that $-\beta_{min}$ and
287 β_{min} are the minimum leading and lagging PF values.

$$288 \quad \sqrt{(P_i^{DG})^2 + (Q_i^{DG})^2} \leq S^{DG} \quad (12)$$

$$289 \quad -\tan(\cos^{-1} \beta_{min}) \cdot P_i^{DG} \leq Q_i^{DG} \leq \tan(\cos^{-1} \beta_{min}) \cdot P_i^{DG} \quad (13)$$

290 where Q_i^{DG} is the reactive DG power injected at the i^{th} node.

291 2.4. PQ Indices

292 In power distribution systems, apart from the functions that describe the objective and
293 constraints that assess the operational performance, there are other indices that evaluate the impacts
294 of the proposed solution on the PQ performance of the studied systems, such as the load balancing
295 index (LBI), and aggregate voltage deviation index ($AVDI$). The mathematical expressions for these
296 quantities are given as follows:

297 2.4.1. Load Balancing Index (LBI)

298 Changing the state of the switches of a distribution system will change its topography. In turn,
299 the loads between the feeders can be distributed to balance the system and avoid the overloading of
300 feeders. In this work, the balancing index (LBI) is used to reflect the loading level of each line in the
301 distribution network [16]. The LBI of the b^{th} line is formulated as follows:

$$LBI_b = \left(\frac{I_b}{I_b^{rated}} \right)^2, \forall b \in N_{br} \quad (14)$$

where I_b is the current flowing in line b and is limited by its rated value I_b^{rated} and N_{br} is the number of lines. Hence, the total load balancing index LBI_{tot} is expressed as the sum of the balancing indices of the lines, thus:

$$LBI_{tot} = \sum_{b=1}^{N_{br}} LBI_b \quad (15)$$

LBI of a certain line decreases if the total load connected to this line decreases, and hence, the line current decreases. However, line currents may increase in other lines, increasing their LBI s. For that, the LBI_{tot} is calculated for all branches to help determine the overall load balancing of all lines in the distribution network.

2.4.2. Aggregate voltage deviation index (AVDI)

Voltage deviation is a measure of the voltage quality in the system. It is formulated as the summation of voltage deviations at all nodes in the system from a reference value of 1 per unit, and it is given as:

$$AVDI = \sum_{i=1}^{N_n} |V_i - 1| \quad (16)$$

where i and N_n are the node number and total number of nodes, respectively. A system with lower $AVDI$ indicates a secure system with reduced voltage violations.

3. Problem Formulation

3.1. Objective Function

The main aim of this work is to minimize the total power loss (P_{loss}^{tot}). The objective function P_{loss}^{tot} is divided into two parts, namely the feeder losses due to current flowing in the lines and the SOP's internal power loss ($P^{SOP-loss}$) as expressed in (17).

$$\text{Min } P_{loss}^{tot} = \sum_{i=1}^{N_n-1} \left(\frac{P_i^2 + Q_i^2}{|V_i|^2} \cdot r_{i,i+1} \right) + \mu \cdot P^{SOP-loss} \quad (17)$$

where $\mu=0$ with no SOP losses considered and $\mu=1$ if SOP losses are considered.

3.2. Constraints and Operation Conditions

In addition to the radiality requirements described in Section II. A, power flow equality given in (4), SOP reactive power limits given in (5), SOP capacity limit given in (6), SOP active power loss given in (8), DG capacity limit given in (11) for the first type and (12) for the second type, and DG reactive power limits given in (13), the following constraints regarding voltage magnitudes, lines thermal capacities and the total reactive power injected by DGs and/or SOPs into the system are expressed, respectively, as follows:

$$V_{min} \leq |V_i| \leq V_{max} \quad (18)$$

$$|I_b| \leq I_b^{rated}, \forall b \in N_{br} \quad (19)$$

$$\sum_{i=1}^{N_{DG}} Q_i^{DG} + \sum_{k=1}^{N_{SOP}} (Q_i^{SOP}(k) + Q_j^{SOP}(k)) \leq \sum_{u=1}^{N_n} Q_u^L \quad (20)$$

where V_{min} and V_{max} represent minimum and maximum voltage limits respectively, and N_{DG} is the number of connected DGs. It should be noted that the total reactive power injected by DGs and SOPs must not exceed the total demand reactive power, as expressed in (20), to avoid the system's over-compensation, and to maintain the PF to be within higher lagging values [37], [38]. Also, no reverse power flow is permitted in the system, as expressed in (21). Otherwise, further precautions should

340 be taken by network operators to control excessive reverse power flows and the associated problems
 341 resulting from high DG penetration levels.

$$342 \quad P_i^L - a \cdot P_i^{DG} - b \cdot P_i^{SOP} - c \cdot P_j^{SOP} \geq 0, \forall i \in N_n \quad (21)$$

343 where a equals 1 in the case of node i connected to a DG unit, b equals 1 in the case of node i
 344 connected to a SOP through feeder I , and c equals 1 in the case of node i connected to a SOP
 345 through feeder J ; otherwise, $a = b = c = 0$.

346 3.3. Search Algorithm

347 The hyper-spherical search (HSS) algorithm was developed by Karami *et al.* in 2014 [39] to solve
 348 nonlinear functions and was further enhanced in 2016 [40] to consider mixed continuous-discrete
 349 decision variables to solve MINLP problems. The DC-HSS has the advantages of fast convergence to
 350 the optimal/near-optimal solutions and good performance in solving mixed continuous-discrete
 351 problems. Therefore, we have used the DC-HSS algorithm to solve our optimization problem.

352 3.3.1. Continuous HSS

353 The population is categorized into two types: particles and sphere-centers (SCs). The algorithm
 354 searches in the inner space of the hyper-sphere to find a new particle position with a better value of
 355 the objective function as follows:

356 **Step 1:** Initialization: the algorithm starts by assigning the population size (N_{pop}), the distance
 357 between the particle and the sphere-center (r), taking into account random values between $[r_{min},$
 358 $r_{max}]$, the number of sphere-centers (N_{SC}), the number of decision variables (N), the probability of
 359 changing the particle's angle (Pr_{angle}), and the maximum number of iterations (Max_{iter}). Then, a
 360 vector of decision variables (x_i) is initialized with random values between $[X_{i_{min}}, X_{i_{max}}]$ by a
 361 uniform probability function. A set equal to N_{pop} containing the objective function values is formed
 362 for each vector, in which each vector of the decision variables $[x_1, x_2, \dots, x_N]$ is named as a particle.
 363 Further, the particles are sorted according to their objective function values, and then the best N_{SC}
 364 particles with the lowest objective function are selected as the initial sphere-centers. The rest of the
 365 particles ($N_{pop} - N_{SC}$) are then distributed among the sphere-centers. Finally, a distribution of the
 366 ($N_{pop} - N_{SC}$) particles among the SCs is performed by the objective function difference (OFD) for each
 367 SC, where the OFD is equal to the objective function of SC (f_{SC}) subtracted from the maximum
 368 objective value of SCs ($OFD = f_{SC} - \max_{SCs} f$). The normalized dominance for each SC is defined as:

$$369 \quad D_{SC} = \left| \frac{OFD_{SC}}{\sum_{i=1}^{N_{SC}} OFD_i} \right| \quad (22)$$

370 A randomly chosen $round\{D_{SC} \times (N_{pop} - N_{SC})\}$ number of particles is assigned to each SC.

371 **Step 2:** Searching: each particle seeks to find a better solution by searching the bounding sphere
 372 whose center is the assigned SC. The radius of this sphere is r . The particle parameters (r and θ) are
 373 changed to perform the searching procedure. The angle of the particle is changed by α , which ranges
 374 between $(0, 2\pi)$ with a probability equal to Pr_{angle} . For each particle, r is changed between $[r_{min},$
 375 $r_{max}]$, where r_{max} can be calculated from (23):

$$376 \quad r_{max} = \sqrt{\sum_{i=1}^N (x_{i,SC} - x_{i,particle})^2} \quad (23)$$

377 After the search for particles, if a new particle position has a lower objective function value than that
 378 of its SC, both the SC and particle will exchange their roles, *i.e.* the particle becomes the new SC and
 379 the old SC becomes the new particle.

380 **Step 3:** Dummy particles recovery: An SC with its particles forms a set of particles.

381 The values of the set objective function (SOF) for each set of particles sort these sets to find the worst
 382 sets, in which dummy (inactive) particles are located. The SOF is given by (24).

$$383 \quad SOF = f_{SC} + (\gamma \cdot mean\{f_{particles\ of\ SC}\}) \quad (24)$$

384 where γ is scalar. If γ is small, SOF will be biased towards f_{SC} , otherwise, SOF will be biased
385 towards $f_{particles\ of\ SC}$.

386 To assign dummy particles to other SCs, two parameters are calculated: the first parameter
387 represents the difference of SOF ($DSOF$) for each set and the second one represents the assigning
388 probability (AP) for each SC. These parameters are expressed as follows:

$$389 \quad DSOF = SOF - \max_{groups} \{SOF\ of\ groups\} \quad (25)$$

$$390 \quad AP = [AP_1, AP_2, \dots, AP_{N_{SC}}] \quad (26)$$

391 Further, a preset number of particles N_{newpar} with the worst function values are exchanged with the
392 new generated N_{newpar} particles. Hence, after several iterations, the particles and their SCs will
393 become close.

394 **Step 4:** Termination: the termination criterion is fulfilled if the number of iterations reaches its
395 Max_{iter} or the difference between the function values of the best SCs is smaller than a pre-set
396 tolerance value.

397 3.3.2. Discrete HSS

398 Like the continuous HSS, the discrete HSS starts with the initialization of particles, but with
399 discrete variables. Solutions are then generated randomly from the discrete variables
400 ($X_{id,min}, X_{id,min} + 1, \dots, X_{id,max} - 1, X_{id,max}$) with a uniform probability. N_{SC} particles with the lowest
401 function values are assigned as SCs. The rest of the particles are distributed among the SCs. Then, the
402 same searching procedure as the continuous HSS is performed. It should be mentioned that the angle
403 α is not considered in the searching procedure of the discrete HSS and the only parameter used is
404 the radius r_d , where r_d is selected between $(r_{d,min}, r_{d,min} + 1, \dots, r_{d,max} - 1, r_{d,max})$. $r_{d,max}$ is
405 calculated as follows:

$$406 \quad r_{d,max} = \sqrt{\sum_{i=1}^N (x_{i_d,SC} - x_{i_d,particle})^2} \quad (27)$$

407 The other steps will be performed as presented in the continuous HSS algorithm.

408 3.3.3. Discrete-continuous HSS (DC-HSS)

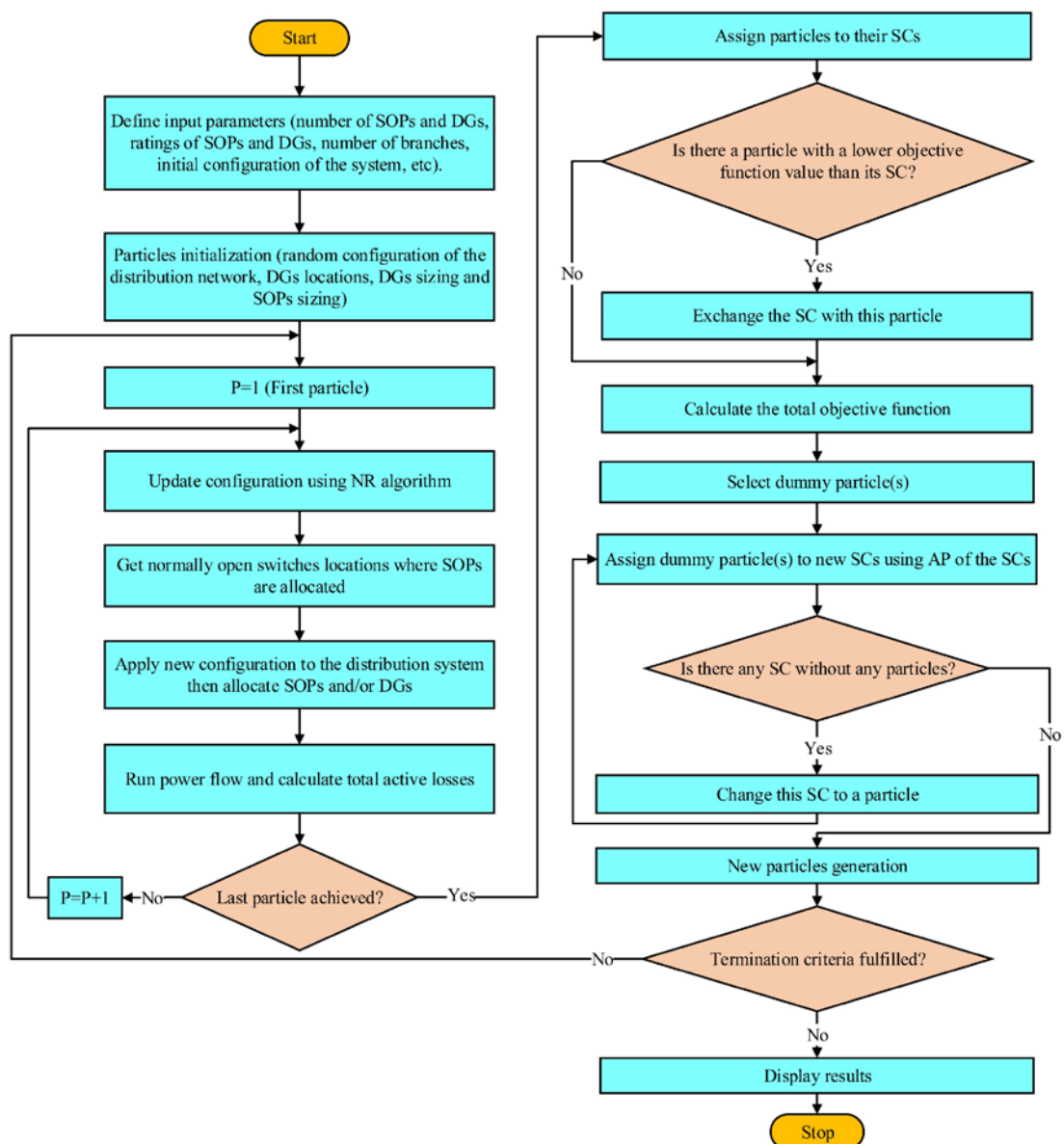
409 DC-HSS combines both continuous and discrete HSS algorithms, in which the particles contain both
410 continuous and discrete variables. The procedure for the continuous variables is structured as
411 presented in the continuous HSS formulation, whilst the procedure for the discrete variables is
412 structured as presented in the discrete HSS formulation. To sum up, the optimization parameters of
413 DC-HSS are as follows: $N_{pop}=1000$, $N_{SC} = 100$, $r_{min} = 0$, $r_{max} = 1$, $r_{d,min} = 0$, $r_{d,max} = 1$, $N_{newpar} =$
414 5 , $Pr_{angle} = 75\%$ and $Max_{iter} = 1000$. Fig. 2 illustrates a comprehensive flowchart for the proposed
415 problem formulation using the DC-HSS algorithm.

416 4. Results and Discussion

417 In this section, the results obtained in the nine scenarios are presented for IEEE 33-node and 83-node
418 systems under different loading conditions. Further, the contribution of SOP loss to the total active
419 power loss as well as the effect of increasing the number of SOPs connected to the systems are studied.
420 Case studies are carried out on an Intel Core i7 CPU, second generation, at 2.2 GHz and 3 GHz
421 maximum turbo boost speed, with 6 GB of RAM with speed 1333 MHz, 6 MB cache memory and
422 contains SSD hard disk at 550 MB per second.

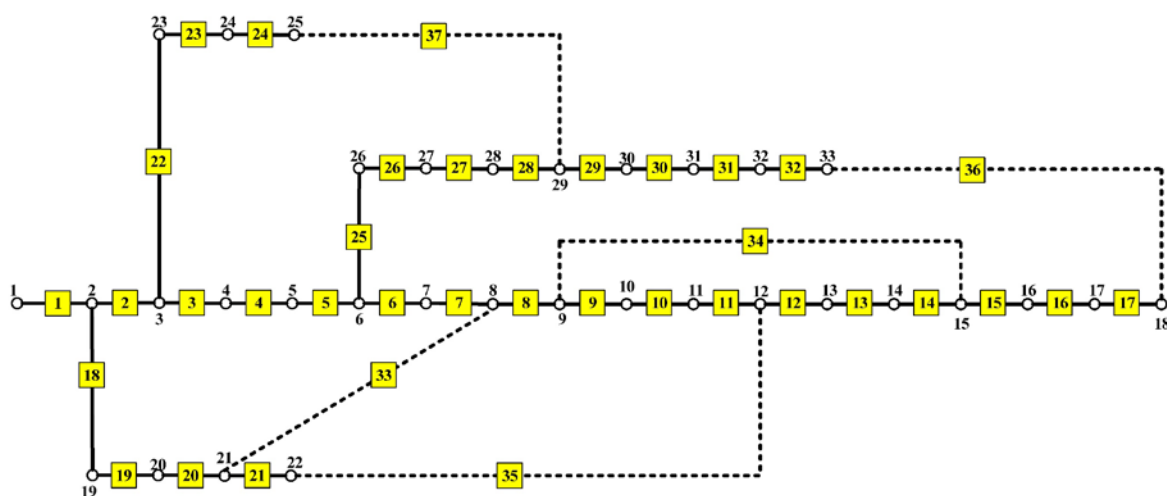
423 4.1. IEEE 33-node distribution system

424 The IEEE 33-node base configuration consists of 32 sectionalized lines and 5 tie-lines as shown in Fig.
425 3. The number of SOPs that can be installed ranges from 1 to 5, *i.e.* $N_{SOP} \in [1,5]$, where the individual
426 SOP rating ($S_I^{SOP} = S_j^{SOP}$) is 1 MVA and A_{loss}^{SOP} equals 0.02 [33], [43], [44]. N_{DG} is set to 3 while S^{DG}



427
428
429

Figure 2. A comprehensive flowchart for the proposed problem formulation using the DC-HSS algorithm



430
431

Figure 3. IEEE 33-node distribution system

432 equals 1 MVA with unity PF. V_{min} and V_{max} values are 0.95 and 1.05 p.u., respectively. Also, I_b^{rated}
 433 is set to 300 A.

434 First, the results obtained for the system in the first three scenarios with no SOPs installed are
 435 given in Table 2.

436 **Table 2.** Total power losses and PQ indices for scenarios 1, 2 and 3: IEEE 33-node system

Loading level	Scenario	P_{loss}^{tot} (kW)	LBI_{tot}	$AVDI$
Light (50%)	1	33.646	0.058	0.678
	2	41.212	0.376	0.862
	3	21.346	0.178	0.500
Normal (100%)	1		NA	
	2			
	3	90.013	0.765	1.064
Heavy (160%)	1			
	2		NA	
	3			

437
 438 On the one hand, the results clarify that optimizing the NR and DGs allocation strategies
 439 separately cannot satisfy the voltage requirements in either the normal or heavy loading conditions,
 440 and only a sub-optimal performance can be achieved in the light loading case. On the other hand,
 441 simultaneous NR and DGs allocation can meet the problem limits in light and normal loading
 442 conditions only. Hence, one can conclude that the first three scenarios cannot guarantee acceptable
 443 performance level of the IEEE 33-node system with loads alteration.

444 Second, the results obtained for scenarios 4 to 9 with lossless SOPs installed in the system are
 445 presented in Table 3 under the three loading conditions.

446 **Table 3.** Total Power Losses and PQ Indices for Scenarios 4 to 9 with Lossless SOPs Installed:
 447 IEEE 33-node system

Scenario	N_{SOP}	Light loading (50%)			Normal loading (100%)			Heavy loading (160%)		
		P_{loss}^{tot} (kW)	LBI_{tot}	$AVDI$	P_{loss}^{tot} (kW)	LBI_{tot}	$AVDI$	P_{loss}^{tot} (kW)	LBI_{tot}	$AVDI$
4	1	38.723	0.343	0.745						
	2	33.686	0.303	0.709		NA				
	3	32.097	0.292	0.701	144.337	1.285	1.085		NA	
	4	29.481	0.271	0.603	143.107	1.255	0.973			
	5	27.420	0.252	0.572	128.576	1.145	1.093			
5	1	23.936	0.211	0.565		NA				
	2	22.323	0.199	0.427	91.206	0.823	0.928		NA	
	3	22.613	0.204	0.444	93.576	0.842	0.969			
	4	22.028	0.205	0.413	89.932	0.833	0.877	269.511	2.317	0.977
	5	22.323	0.209	0.403	89.942	0.832	0.830	267.975	2.275	1.081
6	1	23.709	0.215	0.536	98.803	0.897	1.126			
	2	22.689	0.202	0.464	90.777	0.824	0.931		NA	
	3	23.384	0.213	0.502	90.303	0.839	0.914	254.480	2.228	1.281
	4	22.586	0.205	0.443	89.092	0.823	0.882	255.053	2.255	1.239
	5	23.961	0.204	0.399	89.429	0.853	0.848	258.36	2.220	1.141
7	1	20.548	0.179	0.583						
	2	20.548	0.179	0.583		NA				
	3	19.796	0.175	0.524	87.745	0.759	1.142		NA	
	4	19.454	0.172	0.546	77.212	0.681	1.076			
	5	17.884	0.162	0.512	73.512	0.670	1.050			

Scenario	N_{SOP}	Light loading (50%)			Normal loading (100%)			Heavy loading (160%)		
		P_{loss}^{tot} (kW)	LBI_{tot}	$AVDI$	P_{loss}^{tot} (kW)	LBI_{tot}	$AVDI$	P_{loss}^{tot} (kW)	LBI_{tot}	$AVDI$
8	1	15.299	0.121	0.495		NA			NA	
	2	13.760	0.114	0.428	55.498	0.461	0.822	153.348	1.262	1.261
	3	13.674	0.114	0.443	54.750	0.464	0.785	142.402	1.217	1.221
	4	14.503	0.123	0.416	56.238	0.482	0.798	166.628	1.478	1.302
	5	14.565	0.129	0.387	52.306	0.456	0.764	170.249	1.358	1.141
9	1	14.269	0.122	0.433	57.851	0.508	0.752	160.812	1.412	1.303
	2	13.840	0.118	0.373	51.748	0.445	0.742	144.826	1.265	1.165
	3	13.295	0.116	0.359	49.954	0.448	0.653	125.768	1.133	1.066
	4	11.869	0.110	0.312	50.176	0.444	0.634	137.325	1.241	1.091
	5	12.087	0.106	0.353	45.885	0.433	0.601	122.062	1.131	1.034

448

449

450

451

452

453

454

455

456

457

458

459

On the one hand, the results obtained with one SOP installed in the system with or without NR in the case of no DGs connected exhibit poor performance, which can be explained by the lack of getting an acceptable solution to the problem because of minimum voltage value violation under both the normal and heavy loading conditions, as shown in scenarios 4 and 5. Therefore, to meet the minimum voltage requirement, the reactive power should be compensated by installing additional SOPs, as presented in scenario 6, with 3 to 5 SOPs when NR was considered. On the other hand, the results obtained when DGs were connected into the system without NR (scenario 7) decreased the need for an increasing number of installed SOPs. Further, when NR is enabled, an additional reduction of the number of SOPs is noticed, which will result in reducing the power losses, as revealed by the proposed scenario 9 because it allows freedom in locating SOPs.

460

461

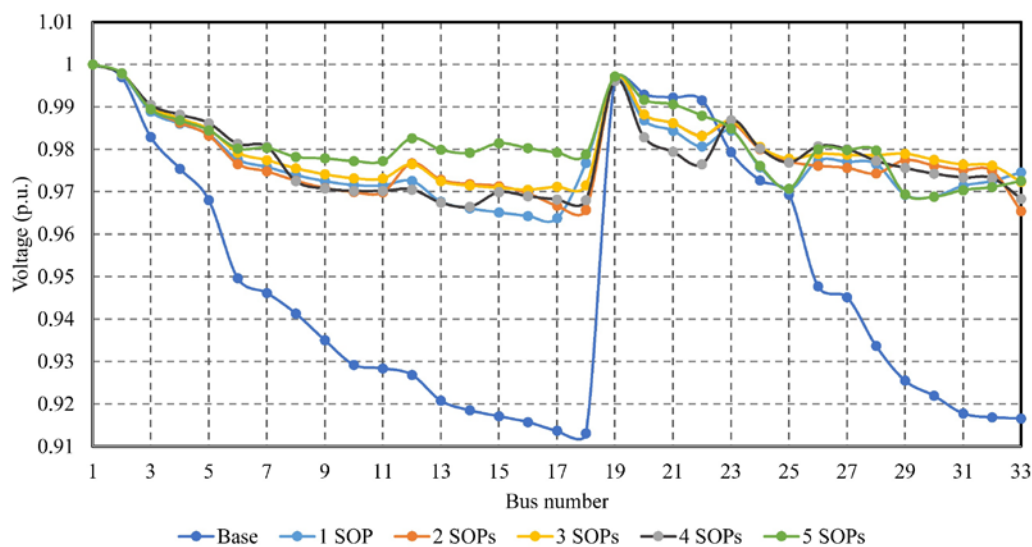
462

463

464

465

To sum up, the results obtained for scenario 9 (simultaneous NR with DGs and SOPs allocation) resulted in the best solutions, highlighted in bold in Table 3, with 5 SOPs at the normal and heavy loading levels and 4 SOPs at the light loading level compared to the results obtained by the other scenarios, in which the power losses are reduced by 74.787% at normal, 77.362% at light, and 78.788% at heavy loading levels with respect to the corresponding base system values. Also, the improvement of the voltage profile obtained in scenario 9 for the system at the normal loading condition is shown in Fig. 4.



466

467

Figure 4. Improvement of the voltage profile at normal loading condition: scenario 9

468

469

Thirdly, the results obtained for scenarios 4 to 9 with the SOPs' internal power losses considered are presented in Table 4 at the three loading levels.

470
471**Table 4.** Total Power Losses and PQ Indices for Scenarios 4 to 9 with SOP Losses Considered:
IEEE 33-node system

Scenario	N_{SOP}	Light loading (50%)			Normal loading (100%)			Heavy loading (160%)		
		P_{loss}^{tot} (kW)	LBI_{tot}	$AVDI$	P_{loss}^{tot} (kW)	LBI_{tot}	$AVDI$	P_{loss}^{tot} (kW)	LBI_{tot}	$AVDI$
4	1	45.414	0.376	0.859						
	2	45.796	0.361	0.819		NA				
	3	35.479	0.292	0.699	177.087	1.099	1.042		NA	
	4	35.083	0.281	0.641	133.125	1.057	1.194			
	5	39.932	0.289	0.635	162.892	1.093	1.049			
5	1	27.184	0.219	0.572		NA				
	2	27.185	0.219	0.573	110.805	0.925	1.147		NA	
	3	30.747	0.209	0.533	113.375	0.887	1.100			
	4	37.655	0.221	0.445	126.837	0.964	0.887	415.433	2.497	0.811
	5	38.209	0.282	0.537	165.753	0.938	1.047	461.002	2.689	0.751
6	1	26.753	0.212	0.526	106.317	0.921	1.125		NA	
	2	26.753	0.212	0.526	104.076	0.881	1.015			
	3	26.754	0.212	0.525	104.774	0.858	0.934	427.952	2.525	1.283
	4	26.824	0.205	0.456	106.070	0.897	1.060	386.968	2.338	1.216
	5	29.629	0.220	0.544	119.559	0.915	1.058	377.700	2.295	1.166
7	1	23.883	0.188	0.592						
	2	27.727	0.201	0.659		NA				
	3	27.669	0.209	0.609					NA	
	4	29.336	0.213	0.632						
	5	36.100	0.234	0.579	114.118	0.783	1.123			
8	1	18.489	0.129	0.502		NA			NA	
	2	18.489	0.129	0.501	68.064	0.509	0.899	204.716	1.131	1.239
	3	19.670	0.118	0.417	72.782	0.494	0.853	196.995	1.279	1.249
	4	29.082	0.129	0.385	86.147	0.508	0.966	317.274	1.712	1.309
	5	25.052	0.129	0.336	94.222	0.578	0.769	220.982	1.289	1.189
9	1	16.828	0.126	0.441	67.019	0.525	0.911		NA	
	2	16.575	0.119	0.375	66.131	0.527	0.804	193.316	1.362	1.322
	3	17.144	0.126	0.446	73.735	0.483	0.782	189.168	1.352	1.238
	4	20.329	0.127	0.390	74.077	0.500	0.746	193.753	1.211	1.029
	5	19.819	0.118	0.408	74.695	0.469	0.602	188.831	1.176	1.135

472

473

474

475

476

477

478

479

480

481

482

483

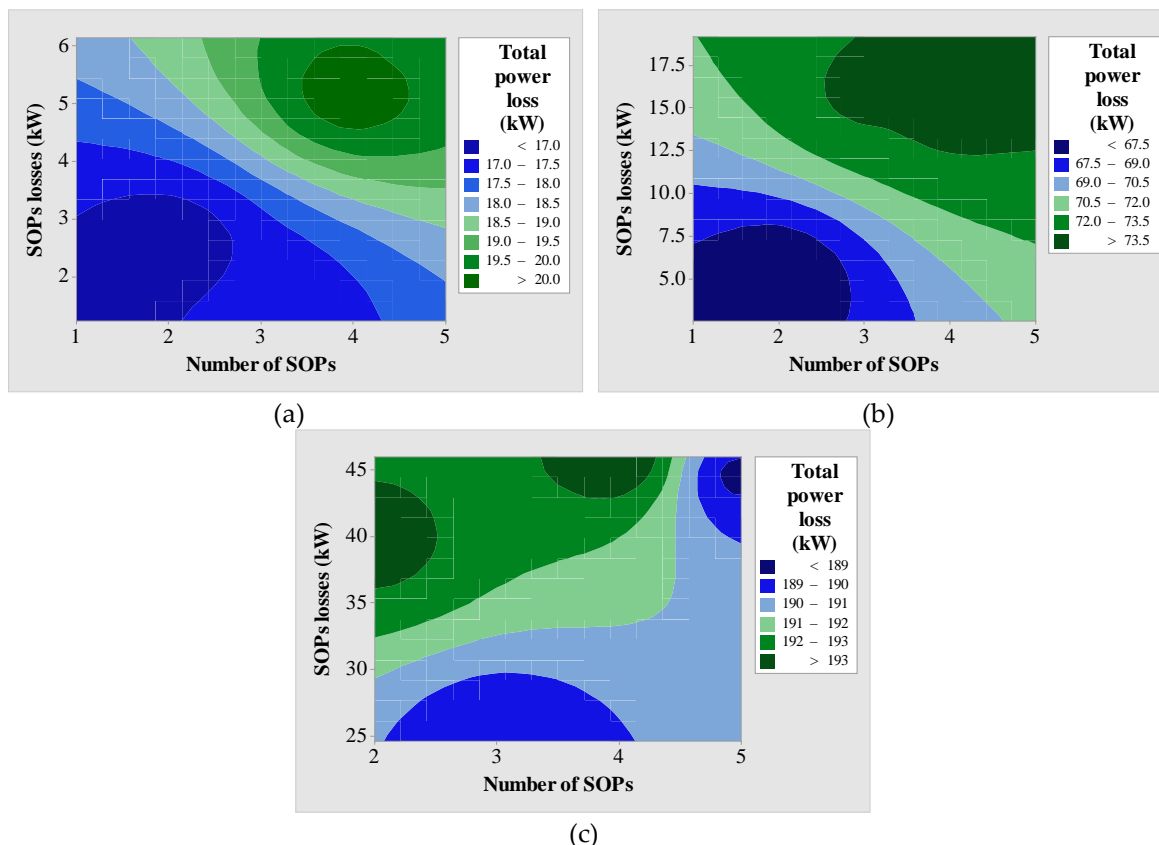
484

485

486

Regardless of economic aspects, in the lossless SOP scenarios, the system with an increased number of installed SOPs becomes more efficient because of the considerable power loss reduction. However, this is not the case if the SOPs' internal losses are considered, because power loss minimization is considerably affected by the SOPs internal losses. This makes clear that loss minimization is not guaranteed by installing more SOPs. In addition, one cannot simply suppose that increasing the number of installed SOPs will increase the SOPs' internal losses proportionally, as this depends on the power transferred by the SOPs and also on the SOPs' locations, as clarified in Fig. 5, with results obtained in scenario 9 that make clear that choosing an appropriate number of SOPs is a matter of optimization. Moreover, after considering the internal power losses of the SOPs, it is obvious that the results obtained for scenario 9 are the best results obtained so far compared to the results obtained for the other scenarios, in which the power losses are reduced by 67.374% using two SOPs at normal, 64.374% using two SOPs at light, and 67.184% using five SOPs at heavy loading levels. All values are given with respect to the corresponding base system values. Furthermore, all the considered PQ indices are enhanced using the same scenario by different values as presented in

487 Table 4, which validates the effectiveness of the proposed solution. The improvement of the voltage
 488 profile obtained in scenario 9 for the system at the normal loading condition with the SOPs' power
 489 loss considered is shown in Fig. 6. A detailed summary of the optimal results obtained for scenarios
 490 4 to 9 at the normal loading condition is given in Tables A.1 and A.2 in the Appendix. Also, the IEEE
 491 33-node system after applying scenario 9 at normal loading condition is shown in Fig. 10. Finally,
 492 optimizing the NR, DGs and SOPs allocation strategies collectively facilitates collaboration between
 493 strategies, which will enable the best performance level of the system to be achieved.

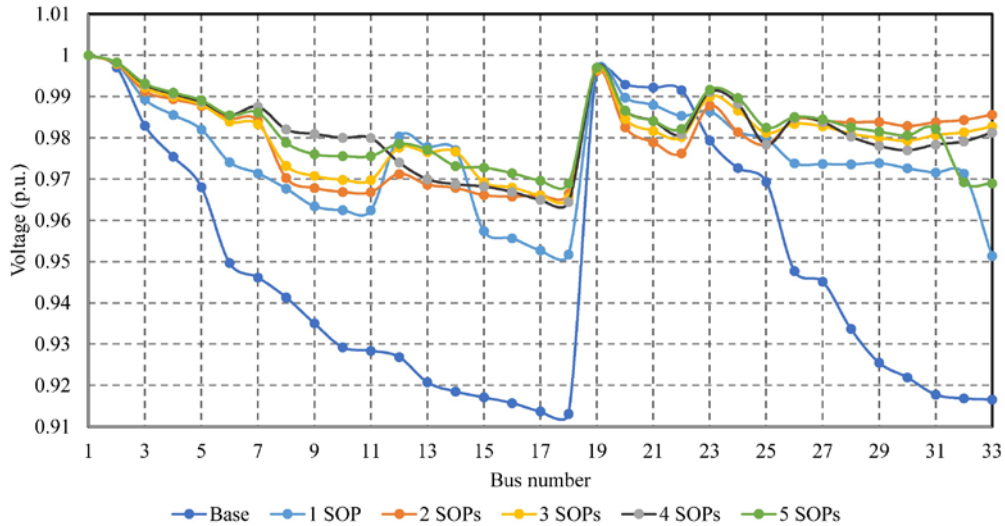


494 **Figure 5.** Contour plots of total power loss versus SOPs losses and N_{SOP} : (a) light loading, (b) normal loading,
 495 and (c) heavy loading.

496 4.2. 83-node distribution system

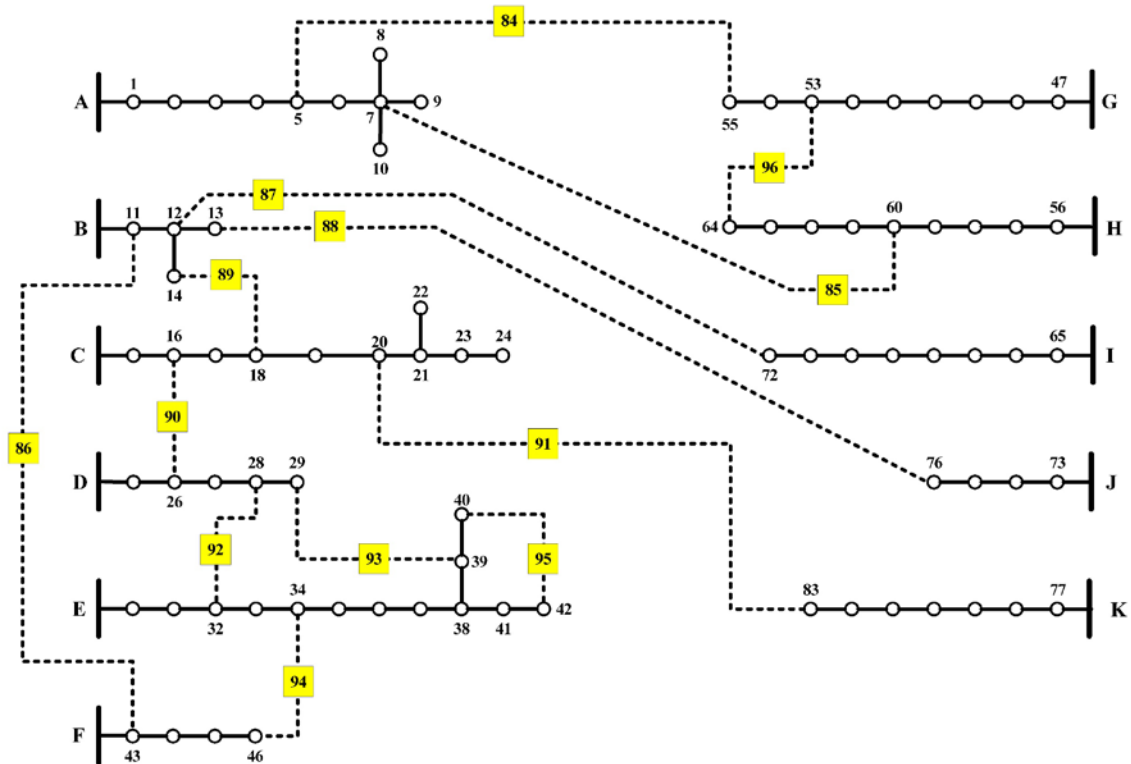
497 In order to validate the effectiveness of scenario 9 proposed in this work, it was examined on an
 498 83-node balanced distribution system from a power company in Taiwan, in which the 83-node base
 499 configuration consists of 83 sectionalized lines and 13 tie-lines as shown in Fig. 7. The number of
 500 SOPs that can be installed ranges from 1 to 5, i.e. $N_{SOP} \in [1,5]$, where the individual SOP rating
 501 ($S_i^{SOP} = S_j^{SOP}$) is 1.5 MVA and A_{loss}^{SOP} equals 0.02 [33], [43], [44]. N_{DG} is set to 8 with S^{DG} equal to 3
 502 MVA and PF ranges from 0.95 lagging to unity. The V_{min} and V_{max} values are 0.95 and 1.05 p.u.,
 503 respectively. Also, I_b^{rated} is set to 310 A.

504
 505
 506



507
508
509
510

Figure 6. Improvement of the voltage profile at normal loading condition with SOPs power loss considered: scenario 9



511
512

Figure 7. The 83-node distribution system

513 First, the results obtained for the system in the first three scenarios with no SOPs installed in the
 514 system are given in Table 5. Once more, the results make clear that optimizing the NR and DGs
 515 allocation strategies separately cannot satisfy the voltage requirements at the heavy loading level,
 516 and only a sub-optimal performance can be achieved at the light and normal loading levels. However,
 517 simultaneous NR and DGs allocation can meet the problem limits considered in the normal and light
 518 loading conditions only. Second, the results obtained for scenarios 4 to 9 with/without SOPs internal
 519 losses in the system are presented in Tables 6 and 7 at the three loading levels.

520

521 **Table 5.** Total power losses and PQ indices for scenarios 1, 2 and 3: 83-node system

Loading level	Scenario	P_{loss}^{tot} (kW)	LBI_{tot}	$AVDI$
Light (50%)	1	113.382	3.237	1.303
	2	97.496	2.713	1.249
	3	87.033	2.425	1.128
Normal (100%)	1	470.241	13.259	2.654
	2		NA	
	3	368.364	10.699	2.309
Heavy (130%)	1			
	2		NA	
	3			

522 **Table 6.** Total power losses and PQ indices for scenarios 4 to 9 without SOP losses: 83-node system

Scenario	N_{SOP}	Light loading (50%)			Normal loading (100%)			Heavy loading (130%)		
		P_{loss}^{tot} (kW)	LBI_{tot}	$AVDI$	P_{loss}^{tot} (kW)	LBI_{tot}	$AVDI$	P_{loss}^{tot} (kW)	LBI_{tot}	$AVDI$
4	1	112.236	3.035	1.163						
	2	107.777	2.929	0.976						
	3	106.452	2.911	0.847		NA				
	4	98.345	2.662	0.958						
	5	99.079	2.697	0.779						
5	1	106.662	3.000	1.213	441.694	12.273	2.501			
	2	103.194	2.898	1.137	427.829	12.010	2.373			
	3	104.861	2.945	1.029	421.891	11.660	2.297		NA	
	4	101.766	2.773	1.062	412.534	11.248	2.171			
	5	96.026	2.769	0.811	390.587	11.017	1.893			
6	1	105.558	3.014	1.034	442.042	12.584	2.293			
	2	100.563	2.878	0.969	425.271	12.106	2.229			
	3	96.450	2.747	0.823	405.221	11.232	2.137			
	4	92.742	2.661	0.825	385.354	10.501	1.836			
	5	89.949	2.484	0.696	407.074	10.428	2.109			
7	1	54.413	1.511	0.895	231.704	6.396	1.879	439.890	12.036	2.773
	2	54.935	1.511	0.887	226.485	6.284	1.614	387.021	10.649	2.325
	3	52.594	1.496	0.680	214.617	6.000	1.668	394.187	10.901	2.233
	4	49.215	1.382	0.688	192.775	5.519	1.464	371.243	10.239	2.214
	5	52.882	1.512	0.632	197.090	5.579	1.562	333.774	9.363	1.816
8	1	60.405	1.797	1.019	253.559	7.358	2.019			
	2	58.648	1.755	0.928	240.294	7.059	1.925			
	3	62.326	1.822	0.899	249.926	7.224	1.979		NA	
	4	57.268	1.679	0.879	243.006	6.816	1.795			
	5	54.513	1.681	0.723	210.822	6.284	1.584			
9	1	51.425	1.456	0.792	219.131	6.282	1.713	379.446	10.806	2.345
	2	49.481	1.382	0.667	203.24	5.821	1.550	345.422	10.022	1.997
	3	46.868	1.321	0.641	192.115	5.392	1.463	348.556	9.905	2.196
	4	43.469	1.238	0.587	189.128	5.084	1.379	345.018	10.815	2.080
	5	45.122	1.309	0.566	189.073	5.140	1.386	302.561	9.163	1.571

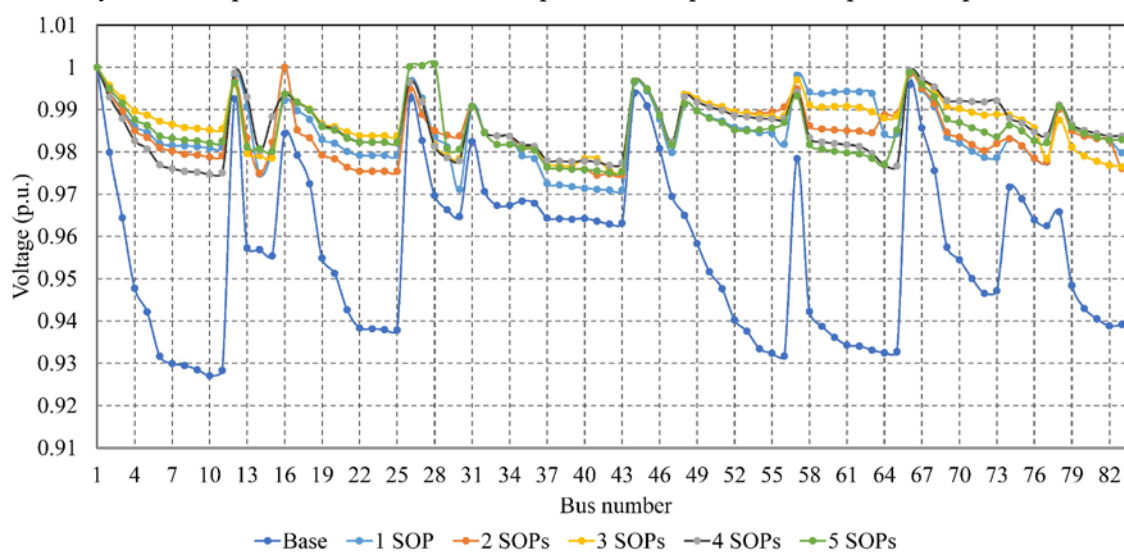
523 From Tables 6 and 7, it can be observed that installing SOPs without NR optimization and DGs
 524 allocation (scenario 4) failed to operate the system within the specified limits, even after increasing
 525 the number of SOPs. On the one hand, for the lossless SOPs cases, scenario 7 succeeded in finding
 526 acceptable solutions for the problem, contrary to scenarios 4, 5, 6 and 8, all of which failed to find an
 527 acceptable solution even with an increased number of SOPs. On the other hand, taking SOPs losses
 528 into account, scenarios 4 to 8 were not capable of finding an acceptable solution for the problem at a
 529 heavy loading level. Still, scenario 9 remains the most successful scenario as it has the ability to
 530 improve the system performance and keep it within the specified limits.

531 **Table 7.** Total power losses and PQ indices for scenarios 4 to 9 with SOP losses considered: 83-node
 532 system

Scenario	N_{SOP}	Light loading (50%)			Normal loading (100%)			Heavy loading (130%)		
		P_{loss}^{tot} (kW)	LBI_{tot}	$AVDI$	P_{loss}^{tot} (kW)	LBI_{tot}	$AVDI$	P_{loss}^{tot} (kW)	LBI_{tot}	$AVDI$
4	1	126.023	3.313	1.349						
	2	134.346	3.219	1.060						
	3	139.039	3.364	1.201				NA		
	4	144.968	3.049	1.279						
	5	145.084	2.893	1.090						
5	1	117.084	3.250	1.287	473.623	12.788	2.610			
	2	119.178	3.170	1.267	478.019	12.783	2.568			
	3	133.988	3.187	1.227	491.723	12.480	2.504			
	4	142.552	2.934	1.188	512.955	12.595	2.374			
	5	145.349	3.024	1.156	518.085	11.919	2.181			
6	1	114.048	3.263	1.278	472.069	13.065	2.646			
	2	116.980	3.218	1.254	470.112	12.527	2.539			
	3	122.259	3.117	1.157	469.115	12.495	2.513		NA	
	4	119.642	3.049	1.163	497.125	12.839	2.593			
	5	116.877	2.939	1.158	502.876	11.627	2.284			
7	1	65.706	1.787	1.078	271.560	6.292	1.969			
	2	81.718	1.531	0.822	286.725	6.845	1.868			
	3	105.414	1.595	0.742	308.381	7.518	1.889			
	4	100.211	1.451	0.719	317.376	5.966	1.637			
	5	115.202	1.432	0.696	343.568	5.853	1.574			
8	1	66.890	1.827	1.039	271.865	7.287	2.058			
	2	77.613	1.909	1.048	310.045	7.159	1.977			
	3	90.195	1.914	1.002	343.867	7.744	2.030			
	4	122.116	1.906	0.972	348.229	7.929	2.073			
	5	154.082	1.918	0.825	344.441	6.647	1.716			
9	1	67.280	1.764	1.043	253.076	6.244	1.836	436.212	11.325	2.654
	2	76.316	1.718	0.888	255.124	6.227	1.836	443.586	10.939	2.389
	3	95.475	1.693	0.942	272.452	5.754	1.737	464.298	11.017	2.451
	4	127.245	1.529	0.924	287.265	5.949	1.758	517.269	11.613	2.551
	5	96.895	1.847	0.976	284.899	6.240	1.619	509.753	10.066	2.306

533 The improvement of the voltage profile obtained in scenario 9 for the system at the normal
 534 loading condition with SOPs power loss considered is shown in Fig. 8. The contribution of SOPs
 535 losses to the total power losses with different numbers of SOPs is clarified in Fig. 9, where the contour
 536 plots agree with the conclusions drawn in the IEEE 33-node case study. A detailed summary of the
 537 optimal results obtained in scenarios 5 to 9 at the normal loading condition is given in Tables A.3 and
 538 A.4 in the Appendix. Also, 83-node system is shown in Fig. 11 after applying scenario 9 at normal
 539 loading condition. Considering the main point, we conclude that the combination of NR, SOPs and
 540 DGs allocation strategies led to the best solution with minimum losses and noticeably enhanced PQ
 541 indices rather than the sub-optimal solutions provided by the individual strategies, particularly at
 542 the different loading levels.

543 In addition, a comparison of the results obtained using the proposed algorithm and the results
 544 obtained using three conventional optimization algorithms presented in previous works [7]: genetic
 545 algorithm (GA), harmony search algorithm (HSA) and modified honeybee mating (MHM), is
 546 conducted to show the effectiveness of the DC-HSS algorithm. The proposed NR methodology is
 547 used in these optimization algorithms to find the optimal/near-optimal solutions of the NR problem
 548 for both the IEEE 33-node and 83-node distribution systems as presented in Tables 8 and 9,
 549 respectively. It can be noted that the optimal/ near-optimal (best) result is obtained using the other
 550 conventional algorithms due to usage of the proposed NR methodology but with a lower
 551 computational time to find the best value compared to the other three algorithms, which validate the
 552 effectiveness of the proposed NR methodology regardless of the optimization technique used.
 553 Finally, the minimum power losses obtained by applying scenario 9 for both the IEEE 33-node and
 554 83-node systems are presented in Table 10 compared to the power loss reported in previous works.



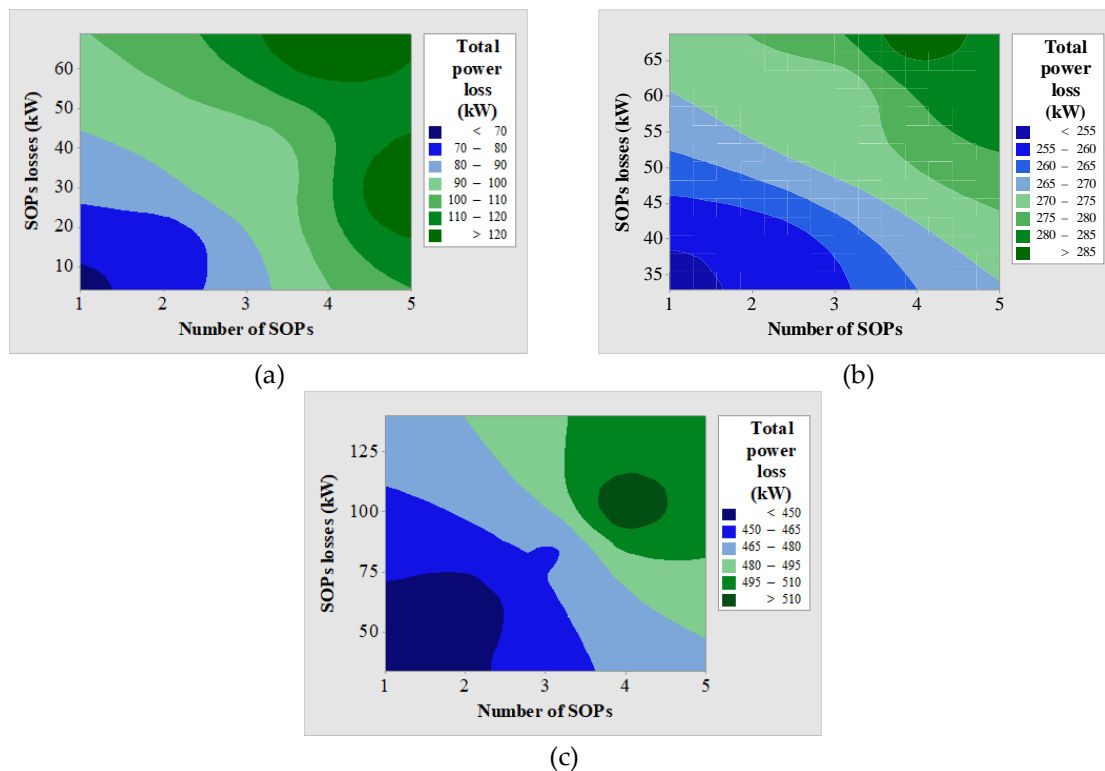
555

556 **Figure 8.** Improvement of the voltage profile at normal loading condition with SOPs power loss
 557 considered: scenario 9

558 5. Conclusion

559 This article presents a multi-scenario analysis of optimal reconfiguration and DGs allocation in
 560 distribution networks with SOPs. The DC-HSS algorithm was used to solve the MINLP of SOPs and
 561 DGs allocation along with NR at different loading conditions to minimize the total power loss in
 562 balanced distribution systems. A new NR methodology is proposed to obtain the possible radial
 563 configurations from random configurations to minimize the power loss in two distribution systems:
 564 the IEEE 33-node and an 83-node balanced distribution system from a power company in Taiwan.
 565 Nine scenarios were investigated to find the best solution that provides the lowest power loss while
 566 improving the system performance and enhancing the PQ measures. The contribution of SOP losses

567 to the total active losses, as well as the effect of increasing the number of SOPs connected to the
 568 system, are investigated at different loading conditions to determine the real benefits gained from
 569 their allocation. It was clear from the results obtained for scenario 9 that simultaneous NR, SOP and
 570 DG allocation into a distribution system creates a hybrid configuration that merges the benefits
 571 offered by radial distribution systems and mitigates drawbacks related to losses, PQ, and voltage
 572 violations while offering far more efficient and optimal network operation. Also, it was found that
 573 the contribution of the internal loss of SOPs to the total loss for different numbers of installed SOPs
 574 is not dependent on the number of SOPs and that loss minimization is not always guaranteed by
 575 installing more SOPs or DGs along with NR. Finally, SOPs can address issues related to voltage
 576 violations, HC, and network losses efficiently to assist the integration of DGs into distribution
 577 systems.
 578



579
 580 **Figure 9.** Contour plots of total power loss versus SOPs losses and N_{SOP} : (a) light loading, (b) normal loading,
 581 and (c) heavy loading.

582 **Table 8.** Results obtained using the proposed and conventional optimization algorithms: IEEE
 583 33-node distribution network

Method	DC-HSS	GA	HSA	MHM
Number of runs	30	30	30	30
Population size	2	2	2	2
Number of iterations	10	10	10	10
Best	139.55	139.55	139.55	139.55
Worst	158.4013	158.4013	158.4013	158.4013
Mean	141.6454	145.6523	151.318	149.1727
Standard deviation	5.766383	5.942117	5.231613	7.353027
Average time (s)	0.3	1	0.3	0.6

584
585**Table 9.** Results obtained using the proposed and conventional optimization algorithms: 83-node distribution network

Method	DC-HSS	GA	HSA	MHM
Number of runs	30	30	30	30
Population size	2	2	2	2
Number of iterations	10	10	10	10
Best	470.241	470.241	470.241	470.241
Worst	509.7132	509.7132	509.7132	509.7132
Mean	475.5788	481.3519	506.4081	488.0029
Standard deviation	8.066826	12.24191	11.59983	12.97165
Average time (s)	0.49	2	0.5	1.7

586

Table 10. Comparison of Previous Works with The Proposed Scenario 9

IEEE 33-node system				83-node system			
Ref.	Year	μ	P_{loss}^{tot} (kW)	Ref.	Year	μ	P_{loss}^{tot} (kW)
[48]	2013	NA	73.050	[45]	1996	NA	383.520
[49]	2009	NA	139.500	[46]	2005	NA	469.880
[50]	2015	NA	72.230	[47]	2014	NA	375.716
	Proposed	0	45.885		Proposed	0	189.073
	Proposed	1	66.131		Proposed	1	253.076

587

588

589

590

591

592

593

594

595

596

597

598

599

600

601

602

603

604

From the analysis conducted to identify opportunities and strategies for reducing network losses through improving system design, and deploying loss-reduction technologies, it is concluded that integrating both DGs and SOPs along with NR simultaneously successfully increased the integration of DGs rather than other scenarios. One of the interesting findings of the manuscript was demonstrating that NR with optimizing tie-lines could reduce active losses considerably. As well, modeling demonstrated that SOPs, installed for the management of constraints in LV feeders, could potentially further reduce losses in modern distribution systems. Further studies will be conducted to integrate that strategy for increasing HC of the distribution systems to accommodate more DGs in balanced and unbalanced distribution systems. It should be noted that a linear power flow formulation can be considered to relax the optimization problem and also to decrease the computational burden.

Another factor that was beyond the framework of the study, and will be included in future studies, is the cost-benefit analysis using a large-scale multi-objective MINLP model of cost and benefits gained by optimal siting and sizing of SOPs and DGs in the engineering practice for large-scale balanced distribution systems. Further, a probabilistic approach is currently conducted to discuss the effectiveness of the proposed deterministic approach while considering seasonality and uncertainty in DGs and demand.

605

606

607

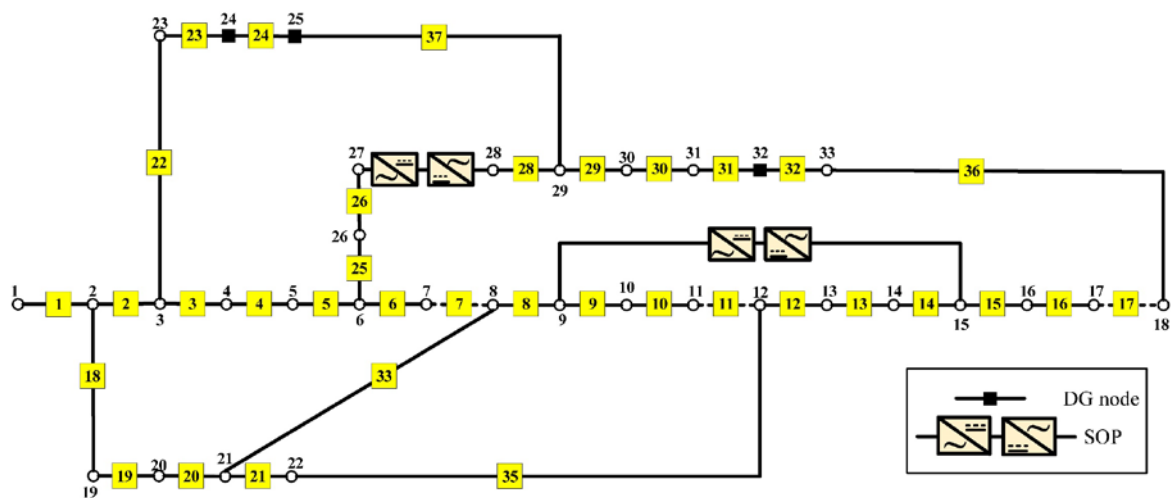
608

Author Contributions: Ibrahim M. Diaaeldin and Shady H.E. Abdel Aleem designed the problem under study; Ibrahim M. Diaaeldin performed the simulations and obtained the results. Shady H.E. Abdel Aleem analyzed the obtained results. Ibrahim M. Diaaeldin wrote the paper, which was further reviewed by Shady H.E. Abdel Aleem, Ahmed El-Rafei, Almoataz Y. Abdelaziz, and Ahmed F. Zobaa.

609

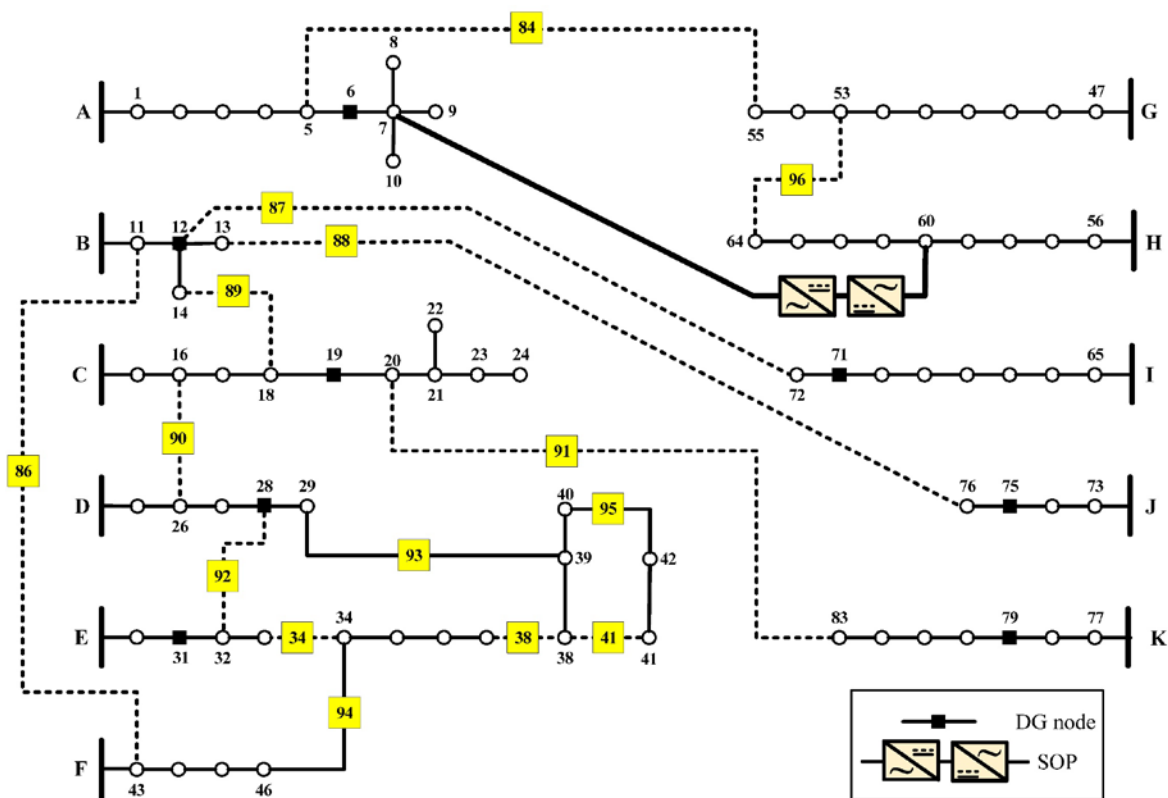
Conflicts of Interest: The authors declare no conflict of interest.

610 Appendix A



611
612
613

Figure 10. IEEE 33-node distribution system after NR, SOPs and DGs allocation with SOPs internal losses considered: scenario 9



614
615
616

Figure 11. 83-node distribution system after NR, SOPs and DGs allocation with SOPs internal losses considered: scenario 9

617 **Table A.1.** Optimal system configuration, sizing and locations of SOPs and DGs for scenarios 4 to 9
 618 without SOPs internal losses at normal loading level: IEEE 33-node distribution system

Scenario	tie-lines	SOPs locations (lines)	SOPs sizing			DG node	DG sizing (MW)
			P_I^{SOP} (MW)	Q_I^{SOP} (MVA _r)	Q_J^{SOP} (MVA _r)		
4	-	33	0.2000	0.0818	0		NA
		34	0	0	0.0933		
		35	0.0600	0.2432	0.6847		
		36	0.0900	0.0344	0.5634		
		37	0	0	0		
5	7	11	0.0450	0.0263	0.0171		NA
		14	-0.0600	0.2924	0.0117		
		32	-0.0600	0.3360	0.1729		
		37	-0.1200	0.2272	0.6886		
6	7	11	0.0450	0	0		NA
		14	0	0	0.0920		
		32	-0.0600	0.3123	0.0885		
		37	-0.1200	0.3670	0.6980		
7	-	33	0	0	0.088	24	0.4200
		34	0	0	0	25	0.4200
		35	0.06	0	0	32	0.2100
		36	0.09	0	0		
		37	-0.0913	0.394984	0.521994		
8	-	7	-0.0131	0	0.173922	24	0.4200
		11	0.045	0	0	25	0.4200
		14	-0.06	0.071586	0	32	0.2100
		32	-0.06	0.366156	0.196486		
		37	-0.12	0.28405	0.521668		
9	-	7	-0.2	0.126	0.06107	24	0.4200
		11	-0.06	0	0	25	0.4200
		28	-0.12	0	0.812957	32	0.2100
		34	-0.06	0.036864	0.077424		
		36	0.09	0.286571	0.239091		

619 **Table A.2.** Optimal system configuration, sizing and locations of SOPs and DGs for scenarios 4 to 9
 620 with SOPs internal losses considered at normal loading level: IEEE 33-node distribution system

Scenario	tie-lines	SOPs locations (lines)	SOPs sizing			DG node	DG sizing (MW)
			P_I^{SOP} (MW)	Q_I^{SOP} (MVar)	Q_J^{SOP} (MVar)		
4	36	33	0.2000	0.0333	0.0538	NA	
		34	-0.0652	0.0066	0.3065		
		35	0.0600	0.1494	0.0480		
		37	-0.1252	0	0		
5	7-11-32	14	0	0	0.1582	NA	
		37	-0.1261	0.0918	0.0138		
6	7-11-32	14	-0.0628	0.0315	0.2978	NA	
		37	-0.1249	0.0009	0.8776		
7	-	33	0	0	0.082994	24	0.4200
		34	-0.06245	0	0.120284		
		35	0.06	0	0	25	0.4200
		36	0.09	0	0	32	0.2100
		37	-0.12568	0.071358	0.166987		
8	7-11-14	32	-0.0624	0	0.1901	24	0.4200
						25	0.4200
		37	-0.1260	0.0853	0.3983	32	0.2100
9	7-11-17	27	-0.0624	0.000293	0.6938	24	0.4200
						25	0.4200
		34	-0.0626	0.0243	0.2831	32	0.2100

621 **Table A.3.** Optimal system configuration, sizing and locations of SOPs and DGs for scenarios 5 to 9
 622 without SOPs internal losses at normal loading level: 83-node distribution System

Scenario	tie-lines	SOPs locations (lines)	SOPs sizing			DG node	DG sizing (MVA)	PF
			P_I^{SOP} (MW)	Q_I^{SOP} (MVA _r)	Q_J^{SOP} (MVA _r)			
5	13-34-39-55- 63-83-86-89	7	-0.4	1.5	0.9757			
		42	0.2	0.4398	0.4719			
		72	0.4184	1.4214	1.3143			
		90	0.3	0.1856	0.5016			
		92	0.7229	0.3661	1.1009		NA	
6	13-34-39-42- 84-86-89-90- 96	72	1.1439	0.3959	1.4468			
		82	-0.1	1.1822	0.3869			
		85	0.4	1.4312	0.6977			
		92	-0.2	1.4781	0.6503			
7	84-86-88-89- 90-91-94-95- 96	85	0.1547	1.492	0.8203	6	1.100	0.9658
						12	1.200	0.9500
		87	0.2941	1.0794	0.7539	19	1.200	0.9500
						28	1.547	0.9817
		92	-0.2	0.9864	1.0761	31	1.799	0.9502
						71	2.000	0.9500
				75	1.200	0.9500		
		93	0.2	0.4686	0.6413	79	2.000	0.9500
8	13-34-39-55- 63-83-86-89	7	-0.4	0.5959	0.7569	6	1.100	0.9747
						12	0.995	0.9503
		42	0.200	0.4948	0.5371	19	1.200	0.9535
						28	1.800	0.9501
		72	0.3509	0.8314	0.3136	31	1.800	0.9501
						71	1.274	0.9501
		90	-0.1	1.2025	1.1796	75	1.200	0.9502
		92	-0.200	0.350	1.3027	79	2.000	0.9501
9	7-13-16-32-34- 72-86-95	38	-0.02	0.239	0.493	6	1.100	0.9509
						12	1.200	0.9502
		55	0.500	1.399	0.804	19	1.200	0.9500
						28	1.782	0.9500
		64	0.300	0.9497	0.576	31	1.678	0.9501
						71	2.000	0.9500
		89	-0.091	0.764	1.236	75	1.200	0.9500
		91	0.300	0.8106	1.033	79	2.000	0.9500

623
624**Table A.4.** Optimal system configuration, sizing and locations of SOPs and DGs for scenarios 5 to 9 with SOPs internal losses considered at normal loading level: 83-node distribution system

Scenario	tie-lines	SOPs locations (lines)	SOPs sizing			DG node	DG sizing (MVA)	PF
			P_I^{SOP} (MW)	Q_I^{SOP} (MVAr)	Q_J^{SOP} (MVAr)			
5	7-13-34-39-42- 55-63-83-86- 89-90-92	72	0.2605	0.4347	0.1784			
		32	-0.208	0.0098	0.5608		NA	
6	7-13-14-34-38- 40-55-63-86-90	82	-0.108	0.1785	1.2975			
		87	-0.209	0.133	1.1108			
						6	1.100	0.9550
7	84-86-87-88- 89-90-91-92- 93-94-95-96	85	0.3367	1.4617	0.4298	12	1.200	0.9500
						19	1.200	0.9500
						28	1.800	0.9500
						31	1.800	0.9905
						71	2.000	0.9500
						75	1.200	0.9500
						79	2.000	0.9505
8	7-13-34-39-42- 55-63-83-86- 89-90-92	72	0.2879	0.4032	0.4376	6	1.100	0.9500
						12	1.200	0.9500
						19	1.200	0.9507
						28	1.800	0.9500
						31	1.800	0.9747
						71	2.000	0.9500
						75	1.200	0.9519
79	2.000	0.9639						
9	34-38-41-84- 86-87-88-89- 90-91-92-96	85	0.2091	1.3189	0.1894	6	1.100	0.9501
						12	1.200	0.9500
						19	1.200	0.9501
						28	1.800	0.9500
						31	1.800	0.9500
						71	2.000	0.9500
75	1.200	0.9500						
						79	2.000	0.9500

625 **References**

- 626 1. Ismael, S.; Abdel Aleem, S.; Abdelaziz, A.; Zobaa, A. Probabilistic hosting capacity enhancement in non-
627 sinusoidal power distribution systems using a hybrid PSO-GSA optimization algorithm. *Energies* **2019**, *12*,
628 1018.
- 629 2. Home-Ortiz, J.M.; Melgar-Dominguez, O.D.; Pourakbari-Kasmaei, M.; Mantovani, J.R.S. A stochastic
630 mixed-integer convex programming model for long-term distribution system expansion planning
631 considering greenhouse gas emission mitigation. *Int. J. Electr. Power Energy Syst.* **2019**, *108*, 86–95.
- 632 3. Zsiborács, H.; Baranyai, N.H.; Vincze, A.; Zentkó, L.; Birkner, Z.; Máté, K.; Pintér, G. Intermittent Renewable
633 Energy Sources: The Role of Energy Storage in the European Power System of 2040. *Electronics* **2019**, *8*, 729.
- 634 4. Sakar, S.; Balci, M.E.; Abdel Aleem, S.H.E.; Zobaa, A.F. Integration of large-scale PV plants in non-
635 sinusoidal environments: considerations on hosting capacity and harmonic distortion limits. *Renew. Sustain.*
636 *Energy Rev.* **2018**, *82*, 176–186.
- 637 5. Chicco, G.; Mazza, A. 100 years of symmetrical components. *Energies* **2019**, *12*, 450.
- 638 6. H.E. Abdel Aleem, S.; T. Elmathana, M.; F. Zobaa, A. Different design approaches of shunt passive harmonic
639 filters based on IEEE std. 519-1992 and IEEE Std. 18-2002. *Recent Patents Electr. Electron. Eng.* **2013**, *6*, 68–75.
- 640 7. Badran, O.; Mekhilef, S.; Mokhlis, H.; Dahalan, W. Optimal reconfiguration of distribution system connected
641 with distributed generations: A review of different methodologies. *Renew. Sustain. Energy Rev.* **2017**, *73*, 854–
642 867.
- 643 8. Elders, I.; Ault, G.; Barnacle, M.; Galloway, S. Multi-objective transmission reinforcement planning
644 approach for analysing future energy scenarios in the Great Britain network. *IET Gener. Transm. Distrib.*
645 **2015**, *9*, 2060–2068.
- 646 9. Ismael, S.M.; Abdel Aleem, S.H.E.; Abdelaziz, A.Y.; Zobaa, A.F. Practical considerations for optimal
647 conductor reinforcement and hosting capacity enhancement in radial distribution systems. *IEEE Access* **2018**,
648 *6*, 27268–27277.
- 649 10. CHEN, S.; LIU, C.-C. From demand response to transactive energy: state of the art. *J. Mod. Power Syst. Clean*
650 *Energy* **2017**, *5*, 10–19.
- 651 11. Qi, Q.; Wu, J.; Zhang, L.; Cheng, M. Multi-Objective Optimization of Electrical Distribution Network
652 Operation Considering Reconfiguration and Soft Open Points. *Energy Procedia* **2016**, *103*, 141–146.
- 653 12. Namachivayam, G.; Sankaralingam, C.; Perumal, S.K.; Devanathan, S.T. Reconfiguration and capacitor
654 placement of radial distribution systems by modified flower pollination algorithm. *Electr. Power Components*
655 *Syst.* **2016**, *44*, 1492–1502.
- 656 13. Kazemi-Robati, E.; Sepasian, M.S. Passive harmonic filter planning considering daily load variations and
657 distribution system reconfiguration. *Electr. Power Syst. Res.* **2019**, *166*, 125–135.
- 658 14. Schnelle, T.; Schmidt, M.; Schegner, P. Power converters in distribution grids - new alternatives for grid
659 planning and operation. In Proceedings of the 2015 IEEE Eindhoven PowerTech; IEEE, 2015; pp. 1–6.
- 660 15. Wang, C.; Song, G.; Li, P.; Ji, H.; Zhao, J.; Wu, J. Optimal siting and sizing of soft open points in active
661 electrical distribution networks. *Appl. Energy* **2017**, *189*, 301–309.
- 662 16. Cao, W.; Wu, J.; Jenkins, N.; Wang, C.; Green, T. Benefits analysis of soft open points for electrical
663 distribution network operation. *Appl. Energy* **2016**, *165*, 36–47.
- 664 17. Zhang, L.; Shen, C.; Chen, Y.; Huang, S.; Tang, W. Coordinated Optimal Allocation of DGs, Capacitor Banks
665 and SOPs in Active Distribution Network Considering Dispatching Results Through Bi-level Programming.
666 *Energy Procedia* **2017**, *142*, 2065–2071.
- 667 18. Long, C.; Wu, J.; Thomas, L.; Jenkins, N. Optimal operation of soft open points in medium voltage electrical
668 distribution networks with distributed generation. *Appl. Energy* **2016**, *184*, 427–437.
- 669 19. Qi, Q.; Wu, J.; Long, C. Multi-objective operation optimization of an electrical distribution network with soft
670 open point. *Appl. Energy* **2017**, *208*, 734–744.
- 671 20. Ji, H.; Li, P.; Wang, C.; Song, G.; Zhao, J.; Su, H.; Wu, J. A strengthened SOCP-based approach for evaluating
672 the distributed generation hosting capacity with soft open points. *Energy Procedia* **2017**, *142*, 1947–1952.
- 673 21. Bai, L.; Jiang, T.; Li, F.; Chen, H.; Li, X. Distributed energy storage planning in soft open point based active
674 distribution networks incorporating network reconfiguration and DG reactive power capability. *Appl.*
675 *Energy* **2018**, *210*, 1082–1091.

- 676 22. Aithal, A.; Li, G.; Wu, J.; Yu, J. Performance of an electrical distribution network with soft open point during
677 a grid side AC fault. *Appl. Energy* **2018**, *227*, 262–272.
- 678 23. Wang, C.; Song, G.; Li, P.; Ji, H.; Zhao, J.; Wu, J. Optimal configuration of soft open point for active
679 distribution network based on mixed-integer second-order cone programming. *Energy Procedia* **2016**, *103*,
680 70–75.
- 681 24. Qi, Q.; Wu, J. Increasing distributed generation penetration using network reconfiguration and soft open
682 points. *Energy Procedia* **2017**, *105*, 2169–2174.
- 683 25. Qi, Q.; Long, C.; Wu, J.; Smith, K.; Moon, A.; Yu, J. Using an MVDC link to increase DG hosting capacity of
684 a distribution network. *Energy Procedia* **2017**, *142*, 2224–2229.
- 685 26. Li, P.; Ji, H.; Yu, H.; Zhao, J.; Wang, C.; Song, G.; Wu, J. Combined decentralized and local voltage control
686 strategy of soft open points in active distribution networks. *Appl. Energy* **2019**, *241*, 613–624.
- 687 27. Yao, C.; Zhou, C.; Yu, J.; Xu, K.; Li, P.; Song, G. A sequential optimization method for soft open point
688 integrated with energy storage in active distribution networks. *Energy Procedia* **2018**, *145*, 528–533.
- 689 28. Thomas, L.J.; Burchill, A.; Rogers, D.J.; Guest, M.; Jenkins, N. Assessing distribution network hosting
690 capacity with the addition of soft open points. In Proceedings of the 5th IET International Conference on
691 Renewable Power Generation (RPG) 2016; Institution of Engineering and Technology, 2016; pp. 1–6.
- 692 29. Guo, X.B.; Wei, W.X.; Xu, A.D. A coordinated optimization method of snop and tie switch operation
693 simultaneously based on cost in active distribution network. In Proceedings of the IET Conference
694 Publications; 2016.
- 695 30. Cao, W.; Wu, J.; Jenkins, N.; Wang, C.; Green, T. Operating principle of soft open points for electrical
696 distribution network operation. *Appl. Energy* **2016**, *164*, 245–257.
- 697 31. Ji, H.; Wang, C.; Li, P.; Zhao, J.; Song, G.; Ding, F.; Wu, J. An enhanced SOCP-based method for feeder load
698 balancing using the multi-terminal soft open point in active distribution networks. *Appl. Energy* **2017**, *208*,
699 986–995.
- 700 32. Ji, H.; Wang, C.; Li, P.; Song, G.; Wu, J. SOP-based islanding partition method of active distribution networks
701 considering the characteristics of DG, energy storage system and load. *Energy* **2018**, *155*, 312–325.
- 702 33. Li, P.; Ji, H.; Wang, C.; Zhao, J.; Song, G.; Ding, F.; Wu, J. Coordinated control method of voltage and reactive
703 power for active distribution networks based on soft open point. *IEEE Trans. Sustain. Energy* **2017**, *8*, 1430–
704 1442.
- 705 34. Wang, C.; Song, G.; Li, P.; Ji, H.; Zhao, J.; Wu, J. Optimal siting and sizing of soft open points in active
706 electrical distribution networks. *Appl. Energy* **2017**, *189*, 301–309.
- 707 35. Xiao, H.; Pei, W.; Li, K. Optimal sizing and siting of soft open point for improving the three phase unbalance
708 of the distribution network. In Proceedings of the 2018 21st International Conference on Electrical Machines
709 and Systems (ICEMS); IEEE, 2018; pp. 2080–2084.
- 710 36. Strategies for reducing losses in distribution networks. Imperial College London. **2018**, [Online]. Available:
711 [https://www.ukpowernetworks.co.uk/losses/static/pdfs/strategies-for-reducing-losses-in-distribution-](https://www.ukpowernetworks.co.uk/losses/static/pdfs/strategies-for-reducing-losses-in-distribution-networks.d1b2a6f.pdf)
712 [networks.d1b2a6f.pdf](https://www.ukpowernetworks.co.uk/losses/static/pdfs/strategies-for-reducing-losses-in-distribution-networks.d1b2a6f.pdf)
- 713 37. El-Fergany, A.A. Optimal capacitor allocations using evolutionary algorithms. *IET Gener. Transm. Distrib.*
714 **2013**, *7*, 593–601.
- 715 38. Abdelaziz, A.Y.; Ali, E.S.; Abd Elazim, S.M. Optimal sizing and locations of capacitors in radial distribution
716 systems via flower pollination optimization algorithm and power loss index. *Eng. Sci. Technol. an Int. J.* **2016**,
717 *19*, 610–618.
- 718 39. Karami, H.; Sanjari, M.J.; Gharehpetian, G.B. Hyper-Spherical Search (HSS) algorithm: a novel meta-
719 heuristic algorithm to optimize nonlinear functions. *Neural Comput. Appl.* **2014**, *25*, 1455–1465.
- 720 40. Ahmadi, S.A.; Karami, H.; Sanjari, M.J.; Tarimoradi, H.; Gharehpetian, G.B. Application of hyper-spherical
721 search algorithm for optimal coordination of overcurrent relays considering different relay characteristics.
722 *Int. J. Electr. Power Energy Syst.* **2016**, *83*, 443–449.
- 723 41. Bloemink, J.M.; Green, T.C. Increasing photovoltaic penetration with local energy storage and soft normally-
724 open points. In Proceedings of the 2011 IEEE Power and Energy Society General Meeting; IEEE, **2011**; pp.
725 1–8.
- 726 42. Bloemink, J.M.; Green, T.C. Benefits of distribution-level power electronics for supporting distributed
727 generation growth. *IEEE Trans. Power Deliv.* **2013**, *28*, 911–919.

- 728 43. Ji, H.; Wang, C.; Li, P.; Ding, F.; Wu, J. Robust operation of soft open points in active distribution networks
729 with high penetration of photovoltaic integration. *IEEE Trans. Sustain. Energy* **2019**, *10*, 280–289.
- 730 44. PCS 6000 for large wind turbines: Medium voltage, full power converters up to 9 MVA. ABB, brochure
731 3BHS351272 E01 Rev. A. **2012**, [Online]. Available: [http://new.abb.com/docs/default-source/ewea-doc/](http://new.abb.com/docs/default-source/ewea-doc/pcs6000wind.pdf)
732 [pcs6000wind.pdf](http://new.abb.com/docs/default-source/ewea-doc/pcs6000wind.pdf)
- 733 45. Peponis, G.J.; Papadopulos, M.P.; Hatziargyriou, N.D. Optimal operation of distribution networks. *IEEE*
734 *Trans. Power Syst.* **1996**, *11*, 59–67.
- 735 46. Chiou, J.-P.; Chang, C.-F.; Su, C.-T. Variable scaling hybrid differential evolution for solving network
736 reconfiguration of distribution systems. *IEEE Trans. Power Syst.* **2005**, *20*, 668–674.
- 737 47. Esmaeili, S.; Dehnavi, H.D.; Karimzadeh, F. Simultaneous reconfiguration and capacitor placement with
738 harmonic consideration using fuzzy harmony search algorithm. *Arab. J. Sci. Eng.* **2014**, *39*, 3859–3871.
- 739 48. Rao, R.S.; Ravindra, K.; Satish, K.; Narasimham, S.V.L. Power loss minimization in distribution system using
740 network reconfiguration in the presence of distributed generation. *IEEE Trans. Power Syst.* **2013**, *28*, 317–325.
- 741 49. Abdelaziz, A.Y.; Mekhamer, S.F.; Badr, M.A.L.; Mohamed, F.M.; El-Saadany, E.F. A modified particle
742 swarm Algorithm for distribution systems reconfiguration. In Proceedings of the 2009 IEEE Power & Energy
743 Society General Meeting; IEEE, **2009**; pp. 1–8.
- 744 50. Rajaram, R.; Sathish Kumar, K.; Rajasekar, N. Power system reconfiguration in a radial distribution network
745 for reducing losses and to improve voltage profile using modified plant growth simulation algorithm with
746 Distributed Generation (DG). *Energy Reports* **2015**, *1*, 116–122.
- 747
748